The Journal of Immunology

Inhibition of Tumor-Induced Myeloid-Derived Suppressor Cell Function by a Nanoparticulated Adjuvant

Audry Fernández, Circe Mesa, Ilaria Marigo, Luigi Dolcetti,
Marilyn Clavell, Liliana Oliver, Luis E. Fernández and
Vincenzo Bronte

Supplementary Material	http://www.jimmunol.org/content/suppl/2010/12/03/jimmunol.100146 5.DC1
References	This article **cites 55 articles**, 25 of which you can access for free at: http://www.jimmunol.org/content/186/1/264.full#ref-list-1

Why *The JI*? Submit online.

- **Rapid Reviews! 30 days*** from submission to initial decision

- **No Triage!** Every submission reviewed by practicing scientists

- **Fast Publication!** 4 weeks from acceptance to publication

*average

Subscription	Information about subscribing to *The Journal of Immunology* is online at: http://jimmunol.org/subscription
Permissions	Submit copyright permission requests at: http://www.aai.org/About/Publications/JI/copyright.html
Email Alerts	Receive free email-alerts when new articles cite this article. Sign up at: http://jimmunol.org/alerts

Inhibition of Tumor-Induced Myeloid-Derived Suppressor Cell Function by a Nanoparticulated Adjuvant

Audry Fernández,* Circe Mesa,* Ilaria Marigo,[†] Luigi Dolcetti,[†,‡] Marilyn Clavell,* Liliana Oliver,* Luis E. Fernández,* and Vincenzo Bronte[†]

The interaction between cancer vaccine adjuvants and myeloid-derived suppressor cells (MDSCs) is currently poorly understood. Very small size proteoliposomes (VSSP) are a nanoparticulated adjuvant under investigation in clinical trials in patients with renal carcinoma, breast cancer, prostate cancer, and cervical intraepithelial neoplasia grade III. We found that VSSP adjuvant induced a significant splenomegaly due to accumulation of CD11b+Gr-1+ cells. However, VSSP-derived MDSCs showed a reduced capacity to suppress both allogeneic and Ag-specific CTL response compared with that of tumor-induced MDSCs. Moreover, splenic MDSCs isolated from tumor-bearing mice treated with VSSP were phenotypically more similar to those isolated from VSSP-treated tumor-free mice and much less suppressive than tumor-induced MDSCs, both in vitro and in vivo. Furthermore, different from dendritic cell vaccination, inoculation of VSSP-based vaccine in EG.7-OVA tumor-bearing mice was sufficient to avoid tumor-induced tolerance and stimulate an immune response against OVA Ag, similar to that observed in tumor-free mice. This effect correlated with an accelerated differentiation of MDSCs into mature APCs that was promoted by VSSP. VSSP used as a cancer vaccine adjuvant might thus improve antitumor efficacy not only by stimulating a potent immune response against tumor Ags but also by reducing tumor-induced immunosuppression. *The Journal of Immunology*, 2011, 186: 264–274.

T umor vaccination is a promising strategy for cancer treatment due to the specificity of response, low toxicity, and induction of long-term memory (1, 2). However, even though there is preclinical evidence for the efficacy of cancer vaccine candidates (3–6), reproducible objective responses in clinical trials are limited (7–10).

The reasons underlying the unsatisfactory clinical responses of cancer vaccines are likely different and not completely established. Tumor-induced immunosuppression is one of the factors contributing to lack of established tumor eradication after immunotherapy (11). Different cell populations with regulatory function are mobilized by tumors contributing to restrain the immune response (12–14). Among these, myeloid-derived suppressor cells (MDSCs) have been described that are able to suppress antitumor immunity through inhibition of CD4+ and CD8+ T cell function (15–18) and control of NK cell cytotoxicity (19, 20). MDSCs are a heterogeneous myelomonocytic population lacking the markers of more mature myeloid cells and commonly expressing both CD11b and Gr-1 markers in mice (12). Suppressive mechanisms of MDSCs require an interplay between the L-arginine metabolizing enzymes arginase (Arg) and NO synthase (Nos) and the Nox family of phagocytic oxidases (21, 22).

Very small size proteoliposomes (VSSP) is an adjuvant based on the combination of outer membrane vesicles (OMPs) from *Neisseria meningitidis* with GM3 ganglioside (23). This product is currently under investigation as part of the formulation of several cancer vaccine candidates at different development stages (4, 24–26). VSSP promotes dendritic cell (DC) maturation, Ag cross-presentation to CD8+ T cells, Th1 polarization, and enhances CTL response (27, 28). However, the capacity of VSSP to influence regulatory cells has not previously been addressed. In this work, we evaluated whether VSSP could modulate the function of tumor-induced MDSCs.

Materials and Methods

Cell lines

MBL-2, EL-4, and EG.7 (EL-4 cell line transfected with the gene encoding for OVA) lymphomas and MCA203 sarcoma are derived from C57BL/6 mice (H-2^b). CT26 is a carcinogen-induced, undifferentiated colon carcinoma derived from BALB/c mice (H-2^d). The C26GM cell line was obtained from C26 colon carcinoma (H-2^d) genetically modified to release GM-CSF (29) and always grown in the presence of 0.8 mg/ml G418 antibiotic (Invitrogen, Milan, Italy).

Mice

Female 8-wk-old C57BL/6 and BALB/c mice were purchased from Harlan (San Pietro al Natisone, Italy) and from the Center for Laboratory Animal Production (Havana, Cuba). Transgenic mice expressing a TCR specific for aa 512–520 from influenza hemagglutinin (HA) presented by H-2K^d (CL4 mice) were a gift from L. Sherman (The Scripps Research Institute, La Jolla, CA). Thy1.1+ congenic mice on BALB/c background and pmel-1 mice expressing transgenic TCRs that recognize gp100$_{25–33}$ peptide in an H-2D^b–restricted manner were provided by N. Restifo (National Cancer Institute, Bethesda, MD). OT-I TCR transgenic mice and CD45.1+ congenic mice on C57BL/6 genetic background were purchased from The Jackson Laboratory (Bar Harbor, ME). CL4 and Thy1.1+ mice were bred to obtain CL4-Thy1.1+ double transgenic mice. All mice were maintained at the animal facilities of Istituto Oncologico Veneto (Padua, Italy) and of the Center of Molecular Immunology (CIM; Havana, Cuba). Animal care and experiments were done according to institutionally approved protocols of Istituto Oncologico Veneto and CIM.

*Center of Molecular Immunology, Havana 11600, Cuba; [†]Istituto Oncologico Veneto, Istituto di Ricovero e Cura a Carattere Scientifico, 35128 Padua; and [‡]Venetian Institute for Molecular Medicine, 35129 Padua, Italy

Address correspondence and reprint requests to Audry Fernández, Immunobiology Division, Center of Molecular Immunology, 216 Street and 15th Avenue, Atabey, Playa, P.O. Box 16040, Havana 11600, Cuba. E-mail address: audry@cim.sld.cu

The online version of this article contains supplemental material.

Abbreviations used in this paper: CIM, Center of Molecular Immunology; DC, dendritic cell; HA, hemagglutinin; HPTLC, high-performance thin-layer chromatography; LN, lymph node; MDSC, myeloid-derived suppressor cell; Nos, NO synthase; OMP, outer membrane vesicle; poly I:C, polyinosinic:polycytidylic acid; TAA, tumor-associated Ag; VSSP, very small size proteoliposomes.

VSSP preparation

VSSP adjuvant was prepared by hydrophobic conjugation of the GM3 ganglioside with the OMP complex from *N. meningitides* strain 385 (Finlay Institute, Havana, Cuba), as described by Estevez et al. (23). Briefly, GM3 and OMP were dissolved in 0.1 M Tris-HCl buffer (pH 8.5), containing sodium deoxycholate and SDS, and then dialyzed to remove detergents. This procedure allowed ganglioside and proteins to hydrophobically incorporate into VSSP and conferred high solubility to the nanoparticulated $(24.7 \pm 1.1 \text{ nm})$ conjugate. GM3 ganglioside was obtained from canine erythrocytes, and purity was monitored by high-performance thin-layer chromatography (HPTLC) (23).

Generation of bone marrow-derived DCs

Bone marrow cells were harvested from femurs and tibias and single-cell suspension cultured in the presence of 20 ng/ml recombinant murine GM-CSF (PeproTech, Rocky Hill, NJ) as described elsewhere (30). Eighteen hours before harvesting, DCs were matured with 1 µg/ml LPS (Sigma, Milan, Italy) and pulsed with the relevant peptide at 2 µg/ml.

CD11b$^+$ cell induction and isolation

BALB/c or C57BL/6 mice were challenged s.c. on day 0 with 5×10^5 and 1×10^6 cells of C26GM and EL-4 tumor lines, respectively. VSSP (CIM) was administered s.c. on days 1, 2, and 7 at 100 µg protein per mouse in BALB/c mice, whereas in C57BL/6 mice the dose was 200 µg protein per mouse on days 4, 5, and 11. In a third tumor model, 1×10^5 cells from MCA203 sarcoma were inoculated s.c. in C57BL/6 mice and VSSP administered on days 11, 12, and 18. Tumor-free mice treated with VSSP and PBS-injected tumor-bearing mice were included as controls. Two days (EL-4 and C26GM tumors), 4 d (MCA203 model), and 7 d (EL-4 model) after the last VSSP inoculation, animals were euthanized, and spleens and tumors were harvested under sterile conditions. Single-cell suspensions were prepared, and MDSCs were isolated using magnetic microbeads conjugated with monoclonal rat anti-mouse/human CD11b Ab (Miltenyi Biotec, Bergisch Gladbach, Germany), following the manufacturer's instructions. Purity of the cell population was evaluated by flow cytometry and exceeded 90%.

FACS analyses

For phenotype characterization, cells were stained with proper amount of specific Abs and their control isotype Abs using conventional protocols. In all cases, cells were previously incubated with anti-mouse FcγR 2.4G2 ascites (HB-197; American Type Culture Collection, Manassas, VA) to reduce the nonspecific binding. Cells were acquired using a FACSCalibur flow cytometer (Becton-Dickinson, Franklin Lakes, NJ) and analyzed with FlowJo 7.2.2 software (Tree Star, Ashland, OR). For intracellular staining, cells were first labeled with Abs against surface Ags, fixed and permeabilized with a Golgi Stop kit according to the manufacturer's protocol (BD Pharmingen, Oxford, U.K.), and then stained for intracellular cytokines or isotype controls. All conjugated Abs were purchased from BD Pharmingen, with the exception of anti-F4/80–FITC (AbD Serotec, Oxford, U.K.) and anti-CD11b–PECy5.5 (eBioscience, Hatfield, U.K.).

In vitro suppression assays

Splenocytes from CL4 or pmel-1 transgenic mice were diluted in gamma-irradiated BALB/c or C57BL/6 splenocytes to achieve 1 and 2% of Ag-specific CD8$^+$ T cells, respectively. Cells (6×10^5) from the effector cell suspension were cultured in 96-well flat-bottom plates (BD Falcon, Oxford, U.K.) with 1 µg/ml specific peptides (IYSTVASSL and KVPRNQDWL from HA and gp100 proteins, respectively). CD11b$^+$ cells were titrated from 24 to 3% of total cells. Alloreactive CTLs were stimulated by incubation of 6×10^5 splenocytes from BALB/c mice with 6×10^5 allogeneic gamma-irradiated splenocytes obtained from C57BL/6 mice. CD11b$^+$ cells were added at 12 and 6% of total (effector and stimulator) cells. To study the influence of Nos and Arg enzymes in the suppressive mechanism of VSSP-derived MDSCs, L-NMMA and Nor-NOHA inhibitors (Calbiochem, San Diego, CA) were added to allogeneic cultures at 0.5 mM and 2 µM final concentrations, respectively.

To evaluate proliferation of effector cells, 2 d after experiment set up, Ag-specific cultures were pulsed with 1 µCi/well [^{3}H]thymidine (Perkin-Elmer, Milan, Italy) for 18 h, and [^{3}H]thymidine incorporation was measured by scintillation counting. The lytic capacity of CTLs was tested after 5 d of culture in a 5-h [^{51}Cr] release assay. Briefly, 2×10^3 target cells, previously pulsed with 100 µCi Na$_2$^{51}CrO$_4$, were added to different effector cell dilutions. The MBL-2 cell line was used as specific target for allogeneic responses, whereas the targets for Ag-specific lysis were HA peptide-pulsed CT26 and gp100 peptide-pulsed MBL-2 cell lines. When present, the percentage of nonspecific lysis of syngeneic cell lines or nonpulsed targets was subtracted. The percentage of specific lysis was calculated from triplicate samples using the formula: $100 \times$ (experimental cpm − spontaneous cpm)/(maximal cpm − spontaneous cpm).

The suppressive capacity of CD11b$^+$ cells isolated from MCA203 tumor-bearing mice, treated or not with VSSP, was studied in an IFN-γ ELISPOT assay. For IFN-γ ELISPOT assays, cellulose-ester membrane microplates (Millipore, Milan, Italy) were coated with mAb R4-6A2 (BD Pharmingen). Both CD8$^+$ and CD11b$^+$ cells were positively selected from the spleens of tumor-bearing mice using magnetic microbeads (Miltenyi Biotec) following the manufacturer's instructions. CD8$^+$ T cells (5×10^4) were stimulated for 72 h with 1×10^5 cells of the MCA203 tumor cell line, and 2×10^4 CD11b$^+$ cells were added as suppressive fraction. Syngeneic MB16F10 cell line was used as negative control. MCA203 and MB16F10 cell lines were previously treated for 16 h with culture supernatant containing 1000 U/ml murine IFN-α (CIM) to increase MHC class I expression and Ag presentation. Plates were washed extensively, and spots were visualized with biotin-conjugated mAb XMG1.2 (BD Pharmingen), alkaline phosphatase-conjugated goat anti-biotin (Vector Laboratories, Peterborough, U.K.), and AP Substrate Kit (Bio-Rad Laboratories, Hempstead, U.K.). The number of spots was counted in triplicate and calculated using an automatic ELISPOT counter (ELISPOT Reader System ELRIFL04; AID, Straßberg, Germany).

Real-time PCR analysis

Total RNA was extracted by TRIzol (Invitrogen) from magnetically purified splenic CD11b$^+$ cells. cDNA were next obtained from total extracted RNA using M-MLV reverse transcriptase (Invitrogen) according to the manufacturer's protocol. TaqMan real-time PCR assay was performed with 20 ng template cDNA on an ABI PRISM 7700 (Applied Biosystems, Milan, Italy). The following genes were evaluated, using specific primers (Applera, Milan, Italy); neuronal *Nos1*; inducible *Nos2* and endothelial *Nos3*. β-Actin and GAPDH were included as housekeeping genes. Data analyses were performed with SDS 2.3 software (Applied Biosystems).

In vivo CD11b$^+$ cell-mediated suppression of specific CD8$^+$ T cells activation

A total of 20×10^6 to 25×10^6 splenocytes (equivalent to 5×10^6 CD8$^+$ T cells previously determined by FACS) from OT-I or CL4-Thy1.1$^+$ transgenic mice were injected i.v. into naive CD45.1$^+$ or BALB/c recipient mice, respectively (Supplemental Fig. 1A, 1B). Two days later, these mice were vaccinated and within 1 h transferred with purified 3×10^6 to 4×10^6 CD11b$^+$ cells from different sources. A second adoptive transference of purified CD11b$^+$ cells was performed on day 4 after vaccination. On day 10 (counting as zero the vaccination day), cells from lymph nodes (LNs) were isolated, restimulated in vitro for 36 h with specific or control peptides, and analyzed for the Ag-specific IFN-γ release by intracellular staining. Different adjuvant or vaccine systems for OVA immunodominant peptide SIINFEKL on the OT-I transgenic model or HA-specific peptide IYSTVASSL for CL4 mice were used to stimulate CD8$^+$ T cells and will be conveniently specified. Specifically, DC vaccination consisted of the injection of 2×10^5 bone marrow-derived DCs previously pulsed with 2 µg of the relevant peptide. Additionally, in other experimental groups vaccination consisted of the immunization with 100 µg peptide emulsified in IFA (Sigma) or mixed with 100 µg VSSP. Every vaccine was administered s.c. in a single dose except for VSSP vaccine, which was administered following the scheme described previously. CD11b$^+$ cells were isolated from C26GM or EL-4 tumor-bearing mice and treated or not with VSSP, as described earlier for the in vitro experiments. One block of the in vivo experiments (Supplemental Fig. 1C) was performed inoculating 1×10^6 EG.7 tumor cells on the CD45.1$^+$ recipient mice, 6 d before vaccination, as a source of natural induced CD11b$^+$ cells. In this particular case, only the first two consecutive doses of VSSP were administered. In those experiments where nonemulsified vaccines were compared, the transferred CD11b$^+$ cells were previously pulsed for 90 min with 2 µg of the relevant peptide.

In vivo differentiation of CD11b$^+$ cells

An total of 5×10^6 CD11b$^+$ cells sorted from EL-4 tumor-bearing CD45.1$^+$ congenic mice was injected i.v. into C57BL/6 recipient mice (Supplemental Fig. 1D). The host mice, with a CD45.2$^+$ phenotype, were previously challenged with 1×10^6 EL-4 tumor cells and injected or not with 200 µg VSSP. Also, naive and tumor-free VSSP-treated recipient mice were used. On day 3 after adoptive transfer, the recipients' spleens, LNs, and tumors were collected, and single-cell suspensions of all organs were analyzed by FACS.

Antitumor activity of VSSP

C57BL/6 mice were s.c. challenged on day 0 with 3×10^5 cells of the EG.7 tumor cell line. Three vaccination systems were tested, OVA/VSSP and

SIINFEKL peptide/VSSP immunization as well as SIINFEKL/IFA control treatment. OVA and SIINFEKL Ags were administered at 50 μg per mouse, whereas VSSP was given at 200 μg protein per mouse. Mouse groups received three doses of each vaccine or PBS, s.c., on days 4, 5, and 11. In a second tumor model, 1×10^6 MCA203 cells were inoculated, s.c., on day 0 in C57BL/6 mice. Vaccination was performed only with VSSP on days 11, 12, and 18 using 200 μg protein per mouse. The largest perpendicular diameters of the resulting tumors were measured with a caliper, and tumor volume was calculated using the formula: $\pi/6 \times \text{length} \times \text{width}^2$.

Isolation and analyses of tumor gangliosides

Primary MCA203 tumors were dissected on day 22 after tumor challenge. Tumor tissue was homogenized and lipids were extracted in chloroform/methanol/water (4:8:3). These extracts were centrifuged (1000 × g, 15 min), and the supernatant was evaporated and dissolved in chloroform/methanol (1:1) for overnight incubation at 4°C. After centrifugation, the supernatant was evaporated and the dry samples dissolved in chloroform/methanol/water (30:60:8) to be applied to a DEAE–Sephadex A-25 column. The acidic lipid fraction was eluted with 0.02 M sodium acetate in methanol. Monosialo gangliosides contained in these fractions were visualized by spraying orcinol reagent and heating at 100°C for 10 min after separation on HPTLC plates.

Statistics

Equality of variances was analyzed with Bartlett's test, and Kolmogorov–Smirnov test was used to verify normal distribution of data. Comparison of spleen weights as well as phenotype of tumor-infiltrating MDSCs and in vivo differentiation of transferred CD11b$^+$ cells at the tumor site was performed with Student t test (two-tailed), using SPSS 10.0 software (SPSS, Chicago, IL). Statistical significance in the comparison of [^{3}H]thymidine incorporation, number of IFN-γ–producing CD8$^+$ T cells by ELISPOT assay, phenotype of MDSCs, and differentiation of transferred CD11b$^+$ cells in the spleen was tested by ANOVA and Tukey tests. Accumulation of CD11b$^+$Gr-1$^+$ cells was analyzed with Student t test or ANOVA and Tukey tests depending on the number of groups. IFN-γ production by adoptively transferred Ag-specific CD8$^+$ T cells in C26GM and EG.7 tumor-bearing mice was compared by Student t test with control (no CD11b$^+$ cell transference or tumor-free mice) receiving the same immunization system. Analysis of IFN-γ secretion corresponding with the in vivo suppression experiment of the EL-4 tumor model was analyzed with ANOVA and Tukey tests. Statistical differences in the migration of transferred CD45.1$^+$CD11b$^+$ cells were detected in the tumor site or in secondary lymphoid organs with Student t test or ANOVA and Tukey tests, respectively. Analyses of tumor volume were performed by ANOVA and Tukey tests for the EG.7 tumor model and by Mann–Whitney U test for MCA203 tumor-bearing mice.

## Results

VSSP recruits CD11b$^+$Gr-1$^+$ cells with poor suppressive capacity

Subcutaneous administration of VSSP induced splenomegaly in BALB/c and C57BL/6 mice, as revealed by the significant ($p \leq 0.001$ and $p \leq 0.01$, respectively) increase in spleen weights after three injections of the adjuvant (Fig. 1A). Further analysis of splenocyte populations in these animals evidenced a relationship between this splenomegaly and the significant ($p \leq 0.01$) increase in CD11b$^+$Gr-1$^+$ cells proportion, from less than 10% of total cell counts in PBS-treated mice to 24.3 ± 4.6% and 29.7 ± 5.8% in BALB/c and C57BL/6 mice treated with VSSP, respectively (Fig. 1B).

A large literature correlated MDSC accumulation in spleens, blood, and tumor environment (12) with tumor-induced immunosuppression (15, 31), therefore the suppressive capacity of CD11b$^+$Gr-1$^+$ cells elicited by VSSP was assessed. Splenic CD11b$^+$ cells, isolated from either tumor-bearing or VSSP-treated mice, were mixed in different proportions with either CL4 or pmel-1 CD8$^+$ T cells specific for influenza HA and gp100 proteins, respectively. After 5 d of culture with cognate peptides, in

FIGURE 1. Effect of VSSP on MDSC induction. BALB/c and C57BL/6 mice were s.c. injected with three doses of VSSP. A and B, Bar graphs represent spleen weights (A) and percentage of CD11b$^+$Gr-1$^+$ cells (B) in the spleens of VSSP-treated mice 2 d after the last dose. Data are expressed as mean of five individual mice ± SD. Statistical analyses were performed with two-tailed t test: **$p \leq 0.01$; ***$p \leq 0.001$. C–F, CD11b$^+$ cells, immunomagnetically sorted from the spleens of VSSP-treated tumor-free mice or from the spleens of either C26GM (C, D) or EL-4 (E, F) tumor-bearing mice, were cocultured for 5 d, at 24 and 12% of total culture cellularity, with transgenic CD8$^+$ T cells stimulated with specific MHC class I immunodominant peptides (HA or gp100 for H2-K^d and H2-D^b, respectively). Cytotoxicity of the different cultures was then evaluated in a 5-h [^{51}Cr] release assay. Data are plotted as percentage of specific lysis (mean value ± SD) at different effector cell dilutions. Results are representative of two experiments with similar results.
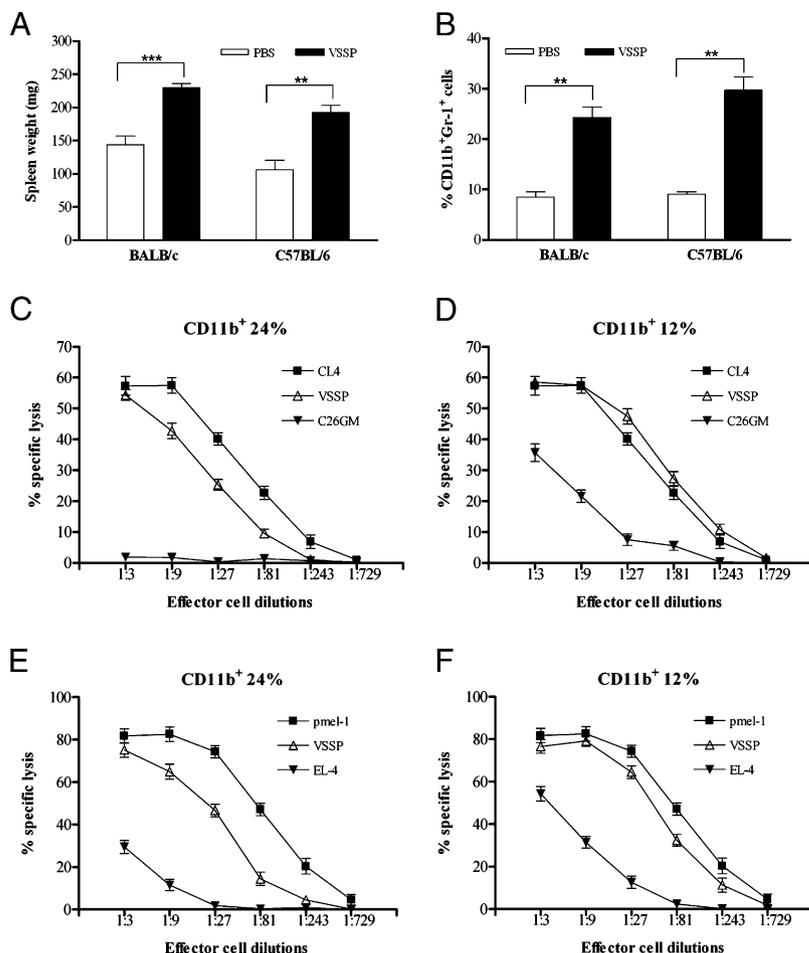
the presence of syngeneic splenocytes as feeder cells, the activity of effector cells was measured in a standard [51Cr] release assay. As shown in Fig. 1C–F, VSSP-induced CD11b+ cells (VSSP-MDSCs) showed a minimal suppressive capacity on Ag-specific T cells compared with that of tumor-induced MDSCs. In fact, CD11b+ cells isolated from animals bearing either EL-4 or C26GM tumors (EL-4–MDSCs and C26GM-MDSCs), added at the final proportion of 24% of total cells in culture, considerably reduced CTL induction, whereas the suppressive action of VSSP-MDSCs was marginal (Fig. 1C, 1E). Accordingly, whereas 12% of EL-4–MDSCs and C26GM-MDSCs still significantly suppressed the generation of cytolytic CD8+ T cells, VSSP-MDSCs were completely inactive (Fig. 1D, 1F).

Furthermore, the inhibition of allogeneic CTLs by VSSP-MDSCs and tumor-induced MDSCs was assessed (Fig. 2A, 2B). Alloantigen-stimulated cytolytic effectors were more susceptible than Ag-specific CTLs to MDSC-mediated suppression, as 12% of C26GM-MDSCs completely abrogated in vitro-generated alloge-neic response, whereas the same tumor-induced MDSC percentage reduced Ag-specific response to a still significant but smaller degree (compare Figs. 1D and 2A). However, even in this setting, VSSP-MDSCs were greatly less suppressive than C26GM-MDSCs when added at both 12 and 6% of total cell numbers (Fig. 2A, 2B).

Nos but not Arg is involved in the residual suppressive capacity of VSSP-derived MDSCs

Arg and Nos enzymes have been related to MDSC suppressive capacity. CD11b+Gr-1+ cells isolated from mice inoculated with EL-4 lymphomas and C26 colon carcinomas depend on these two enzymes to exert their functional activity (15, 32, 33). To find out whether Arg and Nos were contributing to the residual suppression exerted by VSSP-MDSCs, an allogeneic MLR culture was set up adding 12% of CD11b+ cells in the presence of either Nos inhibitor L-NMMA or Arg inhibitor Nor-NOHA (Fig. 2C). After 5 d, a [51Cr] release assay was performed to assess the function of effector cells generated in MLR. L-NMMA completely abrogated the suppressive activity of VSSP-MDSCs. In contrast, Nor-NOHA did not modify the reduced generation of allogeneic cytotoxic splenocytes caused by VSSP-MDSCs (Fig. 2C). These experiments suggest that Nos but not Arg is involved in the residual suppressive capacity of VSSP-MDSCs.

We then attempted to identify which Nos isoform was present in VSSP-MDSCs, comparing the relative expression of *Nos* mRNAs among naive CD11b+ splenocytes and CD11b+ cells from either adjuvant-treated or tumor-bearing mice. Real-time PCR analysis demonstrated that neuronal *Nos* (*Nos1*) gene expression was downregulated in CD11b+ cells isolated from the spleens of both VSSP-treated and C26GM tumor-bearing mice (Fig. 2D) compared with that of BALB/c CD11b+ splenocytes from tumor-free mice. However, upregulation of inducible *Nos* (*Nos2*) was reduced in splenic VSSP-MDSCs in comparison with C26GM-MDSCs (Fig. 2E). On the contrary, the expression of endothelial *Nos* (*Nos3*) was relatively upregulated in VSSP-MDSCs, suggesting that Nos3 might be involved in the suppressive mechanism of these cells (Fig. 2F). Notably, we recently demonstrated that different MDSC subsets showed varying expression of Nos isoforms in C26GM tumor-bearing mice. In fact, the Gr-1high subset did not express Nos2 protein but had an increased *Nos3* mRNA level compared with that of the Gr-1low cell subset. Nevertheless, both subsets were sensitive to Nos inhibitor L-NMMA, supporting
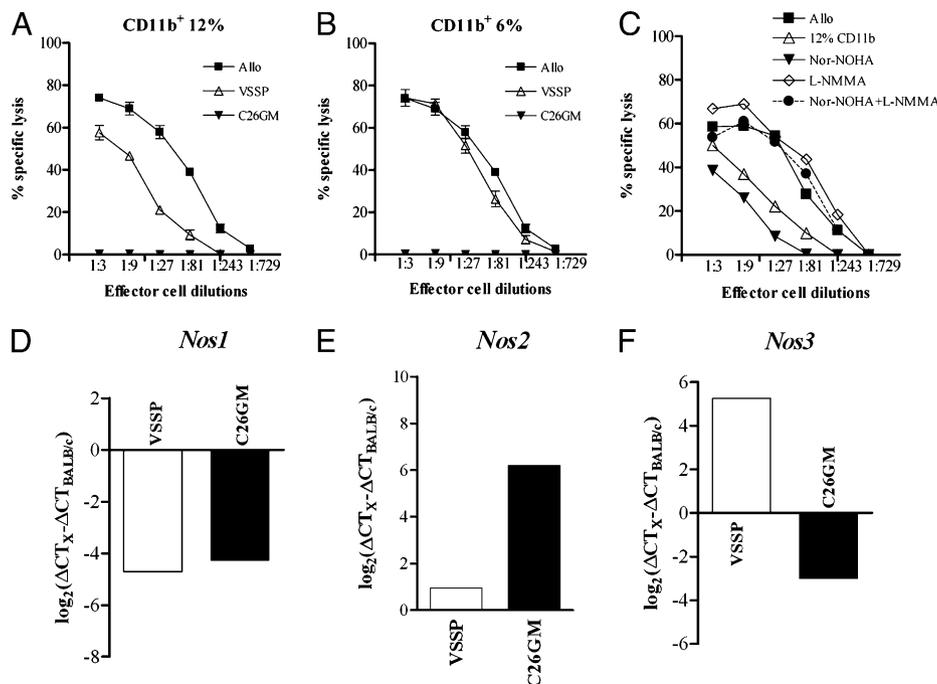

FIGURE 2. Analyses of enzymes involved in the suppressive mechanism of VSSP-derived MDSCs. *A* and *B*, CD11b+ cells were isolated from spleens of VSSP-treated BALB/c mice and titrated in an MLR culture to final proportions of 12 and 6% of total cells. CD11b+ cells isolated from C26GM tumor-bearing were used as positive control of immunosuppression. Cytotoxicity toward allogeneic targets was evaluated 5 d later in a [51Cr] release assay. *C*, Arg and Nos enzymes involvement in the suppressive capacity was evaluated by adding L-NMMA and/or Nor-NOHA inhibitors to the MLR culture performed in the presence of 12% VSSP-MDSCs. Data corresponding with the percentage of specific lysis at different effector cell dilutions are expressed as mean ± SD. MLR experiments were repeated twice. *D–F*, *Nos* gene expression profiles were studied comparatively in splenic CD11b+ cells from VSSP-treated and C26GM tumor-bearing mice by real-time PCR analysis. Graphs show the logarithm of the differences in threshold cycle, corresponding with the *Nos1*, *Nos2*, and *Nos3* genes, between CD11b+ cells in the experimental groups and CD11b+ splenocytes from tumor-free BALB/c mice ($\Delta CT_x - \Delta CT_{BALB/c}$). Real-time analyses were performed with CD11b+ cells from three different experiments with similar results.

the idea that Nos3 could be effective in place of Nos2 in some MDSC subsets (34).

VSSP administration changes the phenotype of MDSCs isolated from the spleens of tumor-bearing mice

The influence of VSSP inoculation on the myeloid populations in tumor-bearing mice was then addressed by administering three doses of VSSP, s.c., to mice previously inoculated with C26GM tumor cells. Splenic MDSCs in mice treated with VSSP accounted for 34.6 ± 5.8% of total splenocytes, similar to the 40.9 ± 2.4% found in the spleens of C26GM tumor-bearing mice. In animals with s.c. growing tumors and treated with VSSP, a higher percentage of MDSCs was detected (61.6 ± 1.5%, $p = 0.002$).

Flow cytometry analyses of CD11b^{+} cells sorted from spleens of these mouse groups showed that VSSP-MDSCs expressed increased levels of CD62L compared with those of the C26GM-MDSCs (Fig. 3A, $p = 0.001$). Notably, CD11b^{+} cells derived from VSSP-treated C26GM tumor-bearing mice (C26GM+VSSP-MDSCs) showed a percentage of CD62L analogous to that of VSSP-MDSCs ($p = 0.939$) but different from that of tumor-induced counterparts ($p = 0.001$). Gr-1 distribution was also different ($p = 0.0001$) be-

tween adjuvant-associated and tumor-induced CD11b^{+} cells, with 15.9 ± 1.3% and 32.8 ± 1.1% Gr-1^{low} subpopulation, respectively (Fig. 3A). VSSP administration in tumor-bearing mice significantly reduced (20.4 ± 0.8%, $p = 0.001$) the percentage of CD11b^{+}Gr-1^{low} cells compared with that of nontreated tumor-bearing mice. IL-4Rα was described as a functional marker for MDSCs (15). We also found higher percentages of F4/80[+]IL-4Rα[high] subpopulation within splenic C26GM-MDSCs (29.1 ± 3.9%), in comparison with the 6.10 ± 0.8% and 8.78 ± 0.2% detected in MDSCs isolated from either tumor-free mice ($p = 0.001$) or C26GM tumor-bearing mice ($p = 0.001$) treated with VSSP (Fig. 3A). Furthermore, double staining with anti-Ly6C and anti-Ly6G Abs showed that MDSCs sorted from C26GM tumor-bearing mice treated with VSSP were phenotypically closer to MDSCs from VSSP-treated tumor-free mice. In particular, the Ly6G^{low}Ly6C^{low} population had different abundance in total CD11b^{+} cells from VSSP-treated mice (either tumor-free or tumor-bearing) and untreated animals implanted with C26GM tumors ($p = 0.0001$ and $p = 0.001$, respectively). In fact, Ly6G^{low}Ly6C^{low} cells represented 7.89 ± 0.6% of VSSP-MDSCs and 10.4 ± 3.9% within C26GM+VSSP-MDSCs compared with 28.1 ± 2.1% in C26GM-MDSCs (Fig. 3A). In tumor-free mice,
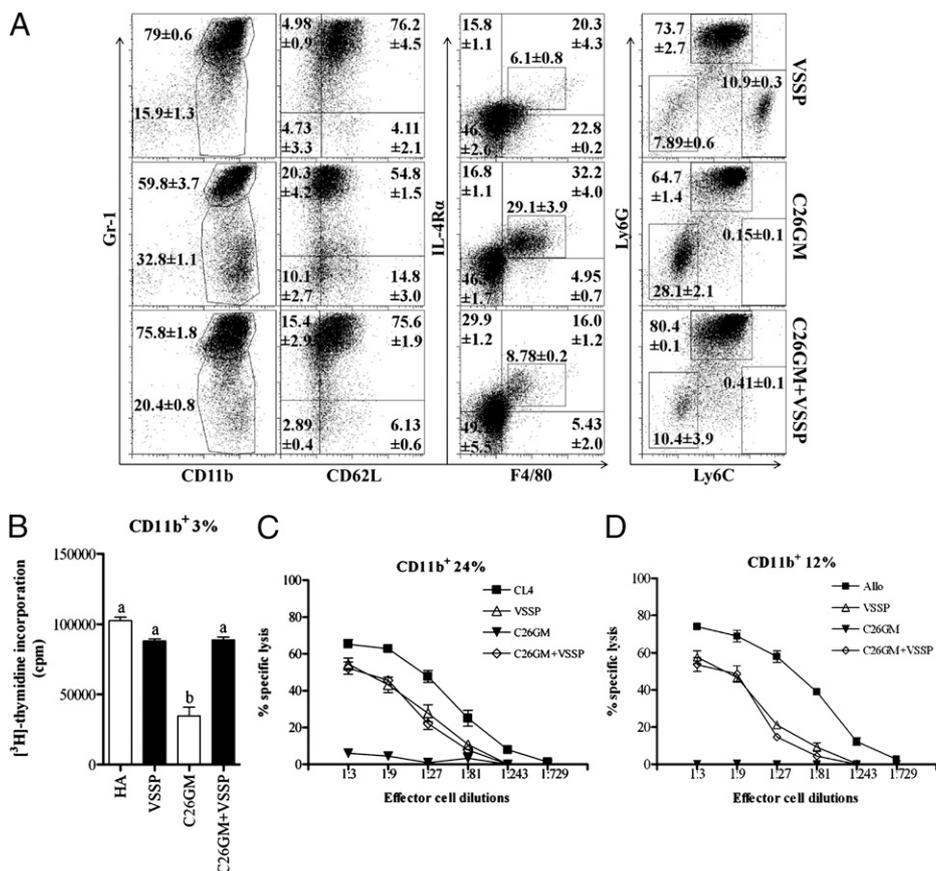

FIGURE 3. Effect of VSSP administration on the phenotype and suppressive capacity of tumor-induced, splenic CD11b^{+} cells. *A*, FACS analysis of relevant markers was performed on MDSCs immunomagnetically enriched from the spleens of VSSP-treated tumor-free, C26GM tumor-bearing, and VSSP-treated C26GM tumor-bearing mice. On the dot plot graphs, quadrants were individually set at positions where isotype control Ab signals were less than 1%. Values on quadrants and gates correspond with the mean ± SD of the cell percentages from three different experiments. *B–D*, Functional suppressive activities of CD11b^{+} cells sorted from the spleen were evaluated by the inhibition of proliferation and cytotoxicity of CD8^{+} T cells. *B*, Bar graph represents proliferative responses of CD8^{+} T cells from CL4 transgenic mice in the presence of CD11b^{+} cells (3% of total cells) and the cognate peptide, measured by [3H]thymidine incorporation. Bars represent mean cpm and SD values, and statistically significant differences are represented by letters (ANOVA and Tukey tests): [a]not significant; [b]$p \leq 0.05$. *C* and *D*, To evaluate cytotoxicity inhibition, either CD8^{+} T cells from CL4 transgenic mice stimulated in the presence of the specific peptide (*C*) or BALB/c splenocytes stimulated with allogeneic C57BL/6 cells (*D*) were used as effector cells. Under these experimental settings, CD11b^{+} cells were added to a final proportion of either 24 or 12% of the total cells, as indicated. Graphs show percentages of specific lysis, measured by [51Cr] release assay, at graded effector cell dilutions, represented as mean ± SD. Data are from one experiment repeated twice with similar results.

VSSP-MDSCs contained ~10.9 ± 0.3% $Ly6G^{low}Ly6C^{high}$ inflammatory monocytes, which were absent in both C26GM-MDSCs and C26GM+VSSP-MDSCs (Fig. 3A).

EL-4–induced $CD11b^+$ cells were also analyzed to corroborate further the phenotypic changes caused by VSSP inoculation in mice from a different genetic background. In this tumor model as well, administration of VSSP increased the number of $CD11b^+Gr-1^+$ cells infiltrating the spleens of tumor-bearing mice, from 14.3 ± 2.4% in untreated animals to 37.4 ± 2.1% in those inoculated with the adjuvant ($p = 0.0001$). Similar to the results obtained in the C26GM tumor model, $CD11b^+$ cells isolated from the spleens of EL-4 tumor-bearing mice (EL-4–MDSCs) showed higher percentages of $Gr-1^{low}$ population ($p = 0.046$) and $F4/80^+IL-4R\alpha^+$ cells ($p = 0.001$) than those of $CD11b^+$ cells coming from adjuvant-injected tumor-bearing mice (EL-4+VSSP-MDSCs) (Supplemental Fig. 2A). In contrast, the percentage of $CD62L^+Gr-1^+$ cells was increased in EL-4+VSSP-MDSCs compared with that of EL-4–MDSCs ($p = 0.001$). Furthermore, $Ly6G^{low}Ly6C^{high}$ inflammatory monocytes accounted for 31.6 ± 1.2% of $CD11b^+$ cells in the spleens of VSSP-treated tumor-inoculated mice, whereas they represented only 19.2 ± 2.3% in untreated animals with EL-4 tumors (Supplemental Fig. 2A; $p = 0.001$).

Suppressive ability of tumor-induced splenic MDSCs is reduced when VSSP is given as adjuvant

To test whether the differences in phenotype between tumor-induced MDSCs, isolated from tumor-bearing mice either treated or not with VSSP, were related to changes in functional activity, a new set of experiments on C26GM and EL-4 tumor models was performed. Initially, we tested the ability of MDSCs to inhibit the proliferation of Ag-specific CL4 $CD8^+$ T cells. Cell proliferation was measured by [³H]thymidine incorporation after stimulation with cognate peptide in the presence of $CD11b^+$ cells. As shown in Fig. 3B, C26GM-MDSCs, at 3% of total cells, showed a higher capacity to suppress proliferation of HA-specific $CD8^+$ T cells than that of $CD11b^+$ cells sorted from VSSP-treated mice, irrespective of the tumor presence.

The same conclusions could be drawn from experiments addressing generation of functional CTLs in vitro. $CD11b^+$ cells, sorted from the spleens of mice, were added during alloantigen or peptide-mediated stimulation of effector cells, and CTL function was evaluated in a [⁵¹Cr] release assay. C26GM-MDSCs induced an almost complete suppression of both HA Ag-specific (Fig. 3C) and alloantigen-specific (Fig. 3D) lytic responses, whereas either VSSP-MDSCs or C26GM+VSSP-MDSCs only partially affected CTL generation, and no difference could be seen among these two groups. Analogous results were obtained with $CD11b^+$ cells purified from EL-4 tumor-bearing mice. Splenic EL-4–MDSCs abolished, almost completely, the lytic activity of Ag-specific $CD8^+$ T cells, and treatment of EL-4 tumor-bearing mice with the adjuvant reduced the inhibitory capacity of the corresponding MDSC population, mimicking the activity of VSSP-MDSCs (Supplemental Fig. 2B). In this model, the effect of VSSP seems to be transient, as 7 d after the last VSSP dose there was a reduction in the VSSP-dependent accumulation of MDSCs; however, MDSCs present in the spleens of EL-4 tumor-bearing mice treated with VSSP still had a reduced suppressive activity on Ag-activated $CD8^+$ T lymphocytes (Supplemental Fig. 3A, 3B).

VSSP prevents in vivo T cell unresponsiveness induced by $CD11b^+$ cells isolated from tumor-bearing mice

To confirm in vivo the modulatory activity of VSSP on tumor-conditioned $CD11b^+$ cells, we performed different adoptive transfer experiments. Basically, in these models Ag-specific $CD8^+$ T cells were adoptively transferred to tumor-free mice that were then vaccinated with the Ag; some of the mice also received an adoptive transfer of tumor-conditioned $CD11b^+$ cells to evaluate their in vivo immunoregulatory function. IFN-γ production by transferred $CD8^+$ T cells was assessed 10 d after vaccination by cytokine intracellular staining.

First, we compared the suppressive capacity of $CD11b^+$ cells isolated from EL-4 tumor-bearing mice treated or not with VSSP, which were transferred to $CD45.1^+$ congenic mice previously injected with OVA-specific $CD8^+$ T cells and vaccinated with SIINFEKL peptide emulsified in IFA. As shown in Fig. 4A and 4B, Ag-specific IFN-γ$^+$ cells were detected in LNs from recipient mice that had received no MDSC injection, whereas the response of LN cells isolated from mice after transfer of EL-4-MDSCs was significantly reduced ($p = 0.013$). In accordance with the in vitro results, $CD11b^+$ cells isolated from VSSP-treated mice, independently of the presence of the tumor, produced no suppression of the IFN-γ secretion in Ag-specific CTLs (Fig. 4A, 4B).

In the second model, the effect of VSSP was evaluated by using it as adjuvant for the HA peptide (IYSTVASSL) formulation to stimulate transferred Ag-specific $CD8^+$ T cells (Fig. 4C, 4D). As a control vaccine, bone marrow-derived, peptide-pulsed DCs were used. In these experiments, adoptively transferred C26GM-MDSCs were still able to suppress Ag-specific $CD8^+$ T cell responses when mice were vaccinated with DCs ($p = 0.027$). However, in recipient mice immunized with VSSP and HA peptide, suppression mediated by C26GM-MDSCs was prevented (Fig. 4C, 4D; $p = 0.086$). In the last model, EG.7 tumor cells expressing OVA were implanted 6 d before vaccination to induce suppressive $CD11b^+$ cells presenting OVA, and the two vaccination approaches discussed before were compared. Fig. 4E illustrates that DC vaccination was prone to EG.7-induced suppression, as IFN-γ production by specific $CD8^+$ T cells was reduced 2-fold in comparison with that of tumor-free mice ($p = 0.001$). In contrast, VSSP vaccination stimulated similar IFN-γ production in tumor-free and EG.7 tumor-bearing mice (Fig. 4E; $p = 0.770$).

The capacity of VSSP to shelter Ag-specific CTL responses in tumor-bearing mice was compared also with polyinosinic:polycytidylic acid (poly I:C) adjuvant, a known inductor of strong $CD8^+$ T cell responses (35, 36). As shown in Supplemental Fig. 4A, immunization with OVA in VSSP generated an in vivo CTL response against SIINFEKL peptide in EL-4 tumor-bearing mice comparable with that observed in tumor-free mice ($p = 0.304$). However, the presence of this MDSC-recruiting tumor significantly reduced the cytotoxic response induced by the administration of three doses of OVA admixed with poly I:C (Supplemental Fig. 4B; $p = 0.008$).

Myeloid populations within the tumor microenvironment are modified by VSSP treatment

Previous experiments have shown that VSSP influenced the functional capacity and phenotype of tumor-induced, splenic MDSCs. To understand whether a similar situation could be found at the tumor site, C26GM tumor-infiltrating $CD11b^+$ cells were isolated from mice either treated or not with VSSP. As shown in Fig. 5A, the expression of CD62L, IL-4Rα, and F4/80 ligands was comparable in both experimental groups. Even the Gr-1 distribution among low and high populations did not change after VSSP inoculation. Notably, tumor-infiltrating as well as splenic MDSCs did not contain a $CD11b^+Ly6G^{low}Ly6C^{high}$ monocytic subpopulation, irrespective of the treatment with VSSP (Fig. 5A). Similar results were obtained with tumor-infiltrating MDSCs from EL-4 tumor-bearing mice inoculated or not with VSSP (Supplemental Fig. 5). The functional capacity of tumor-infiltrating MDSCs was then evaluated in an Ag-specific CTL experimental setting. In contrast with the results obtained in the spleen, treatment with VSSP did not

FIGURE 4. Influence of VSSP on the in vivo suppressive ability of tumor-induced MDSCs. CD8$^+$ T cells from TCR transgenic mice were transferred i.v. into naive congenic recipient mice. Two days later, mice were vaccinated and inoculated i.v. with purified CD11b$^+$ cells from different sources. Ten days later, IFN-γ production on gated, transferred CD8$^+$ T cells was measured. *A* and *B*, Activation of transferred OT-I CD8$^+$ T cells after SIINFEKL/IFA vaccination in mice that were also inoculated with CD11b$^+$ cells isolated from either tumor-free or EL-4 tumor-bearing mice, both treated with VSSP. Mice with no MDSC injection and mice receiving EL-4–MDSC adoptive transfer were used as controls. *C* and *D*, IFN-γ production of transferred CL4 HA-specific CD8$^+$ T cells induced by vaccination with either VSSP-admixed HA peptide or HA peptide-pulsed DCs in the presence or absence of transferred CD11b$^+$ cells isolated from the spleens of C26GM tumor-bearing mice. *B* and *D*, Contour graphs on the right show one representative mouse for each experimental group, and quadrants were individually set at positions where both IFN-γ signals from samples stimulated with control peptide and IgG1/FITC isotype control signals were less than 1%. *E*, The last set of experiments was performed on EG.7 tumor-bearing congenic mice, and the capacity of either SIINFEKL-pulsed DCs or VSSP-admixed SIINFEKL peptide to stimulate IFN-γ secretion by the transferred OT-I CD8$^+$ T cells was compared. Bar graphs (*A*, *C*, *E*) show the IFN-γ–producing cells, per 10^5 CD8$^+$ T cells, as a percentage of the control (mice with no CD11b$^+$ cell transfer or tumor-free mice). Data are represented as mean of three individual mice $\pm$ SD. For *A*, statistical analyses were performed with ANOVA and Tukey tests (different letters represent statistical differences): $^a p > 0.05$; $^b p \leq 0.05$. For *C* and *E*, statistical analyses were performed with two-tailed *t* test: $^* p \leq 0.05$; $^{***} p \leq 0.001$. Two experiments for each setting were performed with similar results.
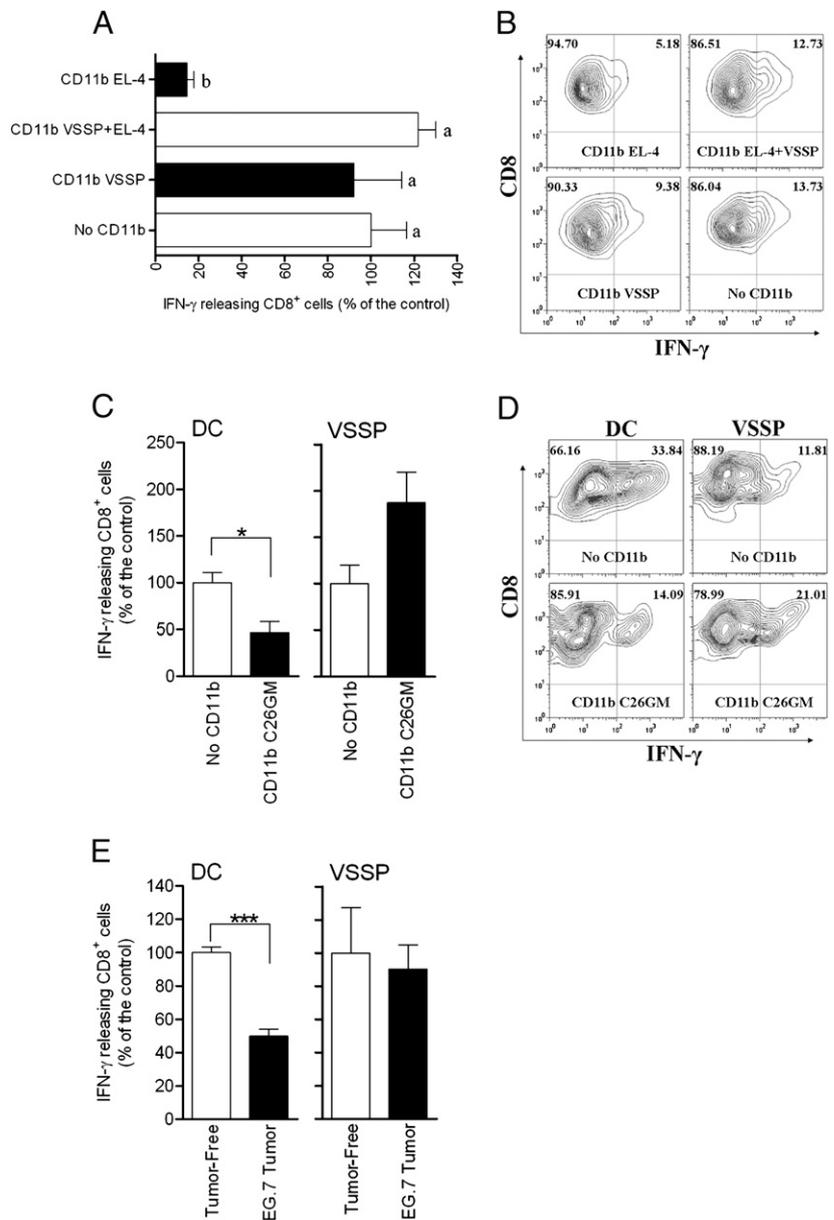
modify the suppression exerted by CD11b$^+$ cells isolated from the tumor (Fig. 5*B*).

Apparently, VSSP administration did not modify, phenotypically and functionally, tumor-induced MDSCs within the tumor microenvironment. However, in experiments where equivalent amount of EL-4-MDSCs, isolated from the spleen, were adoptively transferred into congenic EL-4 tumor-bearing mice, a significant reduction of injected CD45.1$^+$ cells was observed within the tumor in VSSP-treated mice (Fig. 5*C*; $p = 0.001$). This result suggests that VSSP treatment reduces MDSC capacity to infiltrate tumors. In contrast, as shown in Supplemental Fig. 6*A*, a higher number of the transferred CD11b$^+$ cells migrated to LNs in VSSP-treated recipient mice, with nearly 3-fold the amount of CD45.1$^+$ cells observed in both tumor-free ($p = 0.014$) and tumor-bearing ($p = 0.04$) mice. No differences in the migration could be detected in the spleens of treated mice (Supplemental Fig. 6*B*).

Furthermore, in this experimental setting, tumor-infiltrating transferred EL-4-MDSCs were found to be more differentiated into APCs in VSSP-treated congenic mice, as shown by the increased number of transferred cells with high levels of MHC

class II molecules (Fig. 5*D*, $p = 0.05$). Also at the tumor site, a decreased expression of CD11b marker among total MHCII$^+$ CD45.1$^+$ cells was observed (Fig. 5*D*; $p = 0.02$). Moreover, in VSSP-treated tumor-bearing recipient mice, a higher percentage of CD11c$^+$ cells became CD11b$^-$ (Fig. 5*E*; $p = 0.003$), a phenotypic change associated with terminal differentiated mature DCs (37, 38). In the spleen, the percentage of MHCII$^+$F4/80$^+$ macrophages within the transferred population showed no differences between tumor-free and EL-4 tumor-bearing mice, either treated or not with VSSP (Supplemental Fig. 6*C*, 6*E*; $p = 0.889$ and $p = 0.720$, respectively). Nevertheless, a significant increase in total CD11c$^+$ cells, widely employed as a marker of murine DCs (39), was detected in VSSP-treated mice compared with that in both tumor-free mice ($p = 0.022$) and untreated tumor-bearing mice ($p = 0.011$) (Supplemental Fig. 6*D*, 6*F*).

Taken together, these results suggest that VSSP administration reduces the migration of tumor-induced MDSCs toward the tumor site while it accelerates the differentiation of this immature myeloid population into mature APCs within the tumor microenvironment and secondary lymphoid organs.

FIGURE 5. Consequence of VSSP treatment on tumor-infiltrating myeloid populations. EL-4 and C26GM tumor cells were allowed to grow s.c. in C57BL/6 and BALB/c mice, respectively, which were afterward inoculated or not with three doses of VSSP adjuvant. *A*, Nine days after tumor cell inoculation, mice were sacrificed, and tumor-infiltrating CD11b+ cells were isolated and evaluated by FACS. On dot plot graphs, quadrants were individually set at positions where isotype control Ab signals were less than 1%. Values on quadrants and gates correspond with the mean ± SD of the cell percentages from three different experiments. *B*, To evaluate the inhibition of Ag-specific cytotoxicity, CD8+ T cells from CL4 transgenic mice were cocultured, during peptide stimulation, with tumor-infiltrating CD11b+ cells (24% of total cells). Five days later, the lytic capacity of effector cells was tested in a [51Cr] release assay. Graph shows percentages of specific lysis at graded effector cell dilutions, represented as mean ± SD. Data are from one experiment repeated twice with similar results. *C*, Migration ability of MDSCs to the tumor site was also evaluated. CD11b+ cells isolated from the spleens of CD45.1+ EL-4 tumor-bearing mice were adoptively transferred into congenic, CD45.2+ mice bearing EL-4 tumor and either treated or not with VSSP. Dots on graph represent number of transferred CD45.1+ cells (evaluated by FACS) per 10^6 total cells obtained from primary EL-4 tumors. *D* and *E*, Analysis of MHCII+ APCs and particularly MHCII+CD11b− cells, as well as the percentage of CD11c+CD11b− cells, on CD45.1+ gated cells at the tumor site was performed by FACS. Contour graphs show one representative mouse for each experimental group. Statistical differences on dot graphs were detected with two-tailed *t* test: *p ≤ 0.05; ***p ≤ 0.001. Results are representative of two experiments with similar results.
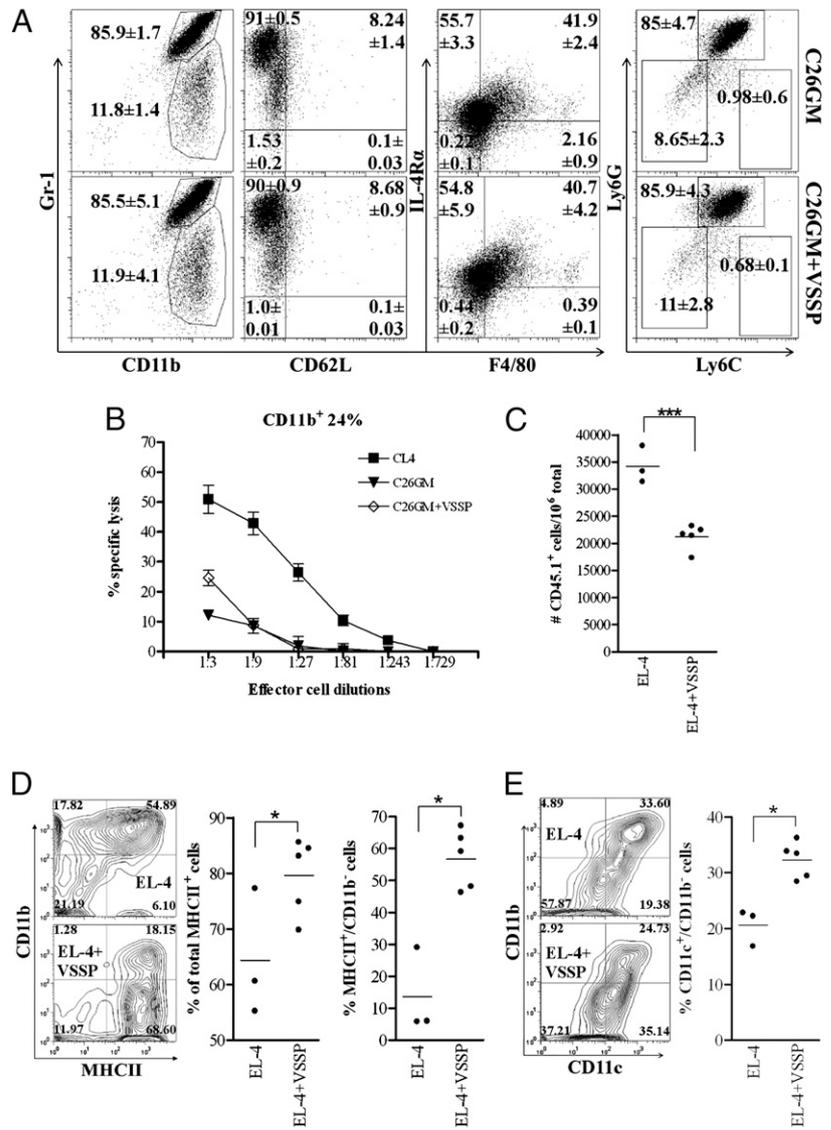
VSSP diminishes the suppression of tumor-specific CTL responses by MDSCs and contributes to reduce tumor growth

We speculated that the effect of VSSP on both splenic and tumor-infiltrating MDSCs might contribute to reduce tumor growth. Indeed, administration of OVA protein or SIINFEKL peptide with VSSP, but not SIINFEKL peptide emulsified in IFA, caused a significant reduction of EG.7 tumor growth in a therapeutic experimental setting (Fig. 6*A*; *p* = 0.01 and *p* = 0.014, respectively), indicating the usefulness of VSSP as adjuvant in tumors triggering an MDSC-dependent immunosuppression.

Furthermore, we decided to study the antitumor effect of VSSP as an adjuvant of a more physiological tumor-associated Ag (TAA). The sarcoma MCA203 is an MDSC-recruiting tumor (15, 34), and GM3 ganglioside was detected in the primary tumor by chemical isolation and HPTLC identification, as shown in Fig. 6*B*. Vaccination of MCA203 tumor-bearing mice with VSSP, which contains GM3 ganglioside, reduced significantly the tumor growth (Fig. 6*B*). This vaccination setting was started on day 11, when s.c. tumors were palpable, indicating a therapeutic effect of VSSP using GM3 as the nominal Ag. In this tumor model as well, VSSP administration increased significantly the frequency of CD11b+Gr-1+ cells in the spleens of tumor-bearing mice (Fig. 6*C*; *p* = 0.0001). To evaluate whether VSSP immunization reduced the capacity of

tumor-induced MDSCs to suppress the response of CD8+ T cells specific to MCA203 tumor Ags, both CD8+ and CD11b+ cells were purified from the spleens of tumor-bearing mice, either treated or not with VSSP, and used in an IFN-γ ELISPOT assay. As shown in Fig. 6*D*, CD8+ T cells isolated from MCA203 tumor-bearing mice [CD8(T)] did not produce IFN-γ when stimulated with MCA203 tumor cells, regardless of the addition of MDSCs. However, VSSP vaccination of tumor-bearing mice caused a significant increase (*p* = 0.0001) in the frequency of IFN-γ–producing, MCA203 Ag-specific CD8+ T cells [CD8(T+V)]. These results suggest the in vivo activation of effector cells specific for other TAAs, an Ag-spreading probably caused by the initial response against GM3 ganglioside. Notably, CD11b+ cells isolated from tumor-bearing mice treated with VSSP [MDSCs(T+V)] showed a significantly reduced suppression on CD8+ T cells derived from VSSP-treated mice [CD8(T+V)] stimulated with MCA203 cells compared with that of tumor-induced MDSCs [MDSC(T)] (Fig. 6*D*; *p* = 0.003). No IFN-γ response was detected after stimulation of both CD8(T) and CD8(T+V) cells with syngeneic MB16F10 tumor cells, indicating the Ag specificity of the response (data not shown). These results indicate that VSSP administration in MCA203 tumor-bearing mice reduced the suppression exerted by tumor-induced MDSCs on CD8+ T cells specific for TAAs and generated an efficient antitumor
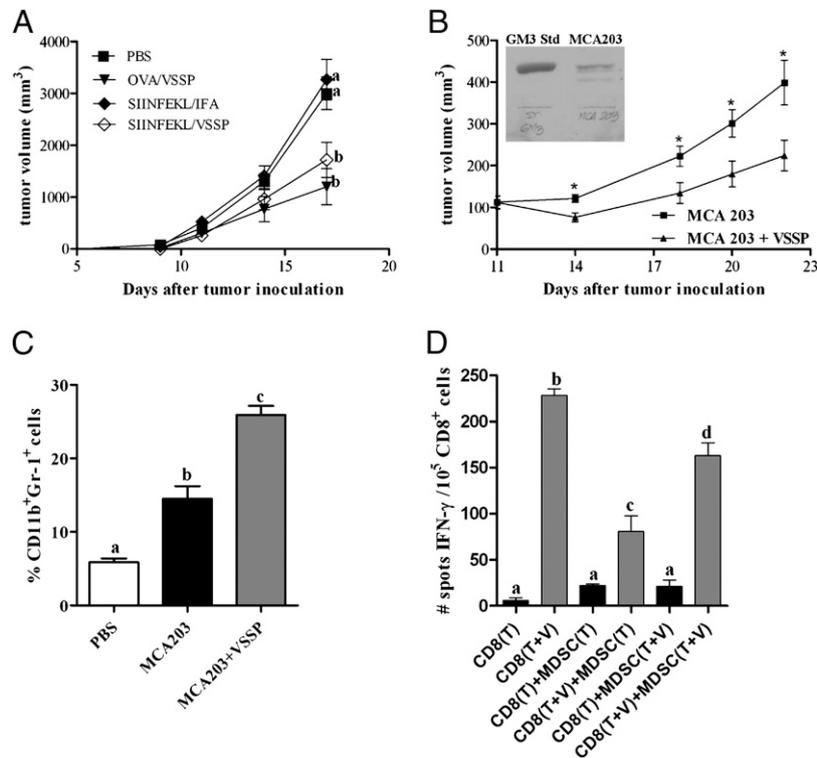
FIGURE 6. Antitumor responses induced by VSSP-based vaccines on MDSC-recruiting tumors. *A*, C56BL/6 mice were s.c. challenged with 3×10^5 cells of the EG.7 tumor cell line on day 0 and subsequently received three doses of OVA/VSSP, SIINFEKL/VSSP, SIINFEKL/IFA, or PBS on days 4, 5, and 11. *B*, MCA203 tumor-bearing C56BL/6 mice were immunized with three doses of VSSP on days 11, 12, and 18 after tumor inoculation. Image inside the graph corresponds with chemical GM3 ganglioside detection by orcinol reagent on MCA203 primary tumors. Graphs *A* and *B* represent tumor volume (mean $\pm$ SD) of 10 individual mice per group at different time points. Statistically significant differences are indicated by diverse letters or by asterisk. *A*, ANOVA and Tukey tests: $^a p > 0.05$; $^b p \leq 0.05$. *B*, Mann–Whitney U test: $^* p \leq 0.05$. *C*, Percentage of CD11b$^+$Gr-1$^+$ cells in the spleens of MCA203 tumor-bearing mice, treated or not with VSSP, 4 d after the last VSSP dose. Data are expressed as mean of five individual mice $\pm$ SD and statistically significant differences ($p \leq 0.001$) are represented by letters (ANOVA and Tukey tests). *D*, The effect of VSSP immunization on the suppression of TAA-specific CTL responses by tumor-induced MDSCs was evaluated in an IFN-γ ELISPOT assay. CD8$^+$ T cells and CD11b$^+$ cells were positively selected from the spleens of MCA203 tumor-bearing mice either treated or not with VSSP. Purified CD8$^+$ T cells were next stimulated for 72 h with MCA203 tumor cell line, and splenic CD11b$^+$ cells were added as suppressive fraction. Bars represent mean and SD values of the number of IFN-γ spots per 10^5 CD8$^+$ T cells. Diverse letters indicate statistically significant differences by ANOVA and Tukey tests (p values are specified in the *Results*). These experiments were repeated twice with similar results.

CTL response against MCA203 tumor, even when the nominal Ag in the vaccine was the GM3 ganglioside.

Discussion

Adjuvants have been frequently used in cancer vaccines to potentiate antitumor immune response. However, some adjuvants can induce MDSC accumulation into tumor-bearing mice and cancer patients. For example, whereas low doses of GM-CSF potentiate antitumor activity, higher doses impaired efficacy of antitumor vaccines through MDSC accumulation (40, 41). These findings highlight the importance of studying the immune modulatory mechanisms of cancer vaccine adjuvants. VSSP is an adjuvant developed at CIM that has been used in a randomized phase II clinical trial on renal carcinoma patients and in three phase I clinical trials on breast cancer, hormone-sensitive prostate cancer, and cervical intra-epithelial neoplasia grade III (unpublished data). Notably, some of these clinical tumors have been associated with the recruitment of MDSCs, for instance breast cancer, renal carcinoma, and prostate cancer (42–44).

In this work, we demonstrated that VSSP adjuvant is able to recruit CD11b$^+$Gr-1$^+$ cells in the spleens of treated mice. Association between infection and CD11b$^+$Gr-1$^+$ cell recruitment has been reported: *Trypanosoma cruzi* and *Taenia crassiceps* infections are linked with T cell unresponsiveness mediated by immature CD11b$^+$

Gr-1$^+$ cells (45, 46). Because VSSP contains bacterial molecules, we presumed that it could induce MDSCs through the physiological mechanisms responsible for the control of anti-infectious response. Another important component of VSSP is GM3 ganglioside. Gangliosides inhibit DC differentiation, and they have been linked to MDSC accumulation (47, 48). The expansion of MDSCs after VSSP inoculation appears to depend on both bacterial and GM3 molecules, because outer membrane vesicles from *N. meningitidis* without the ganglioside recruited a smaller number of MDSCs than did VSSP (Supplemental Fig. 7*A*, 7*B*).

Notably, the splenic CD11b$^+$Gr-1$^+$ population induced by VSSP had a lower capacity to suppress Ag-specific CTL response than that of tumor-induced MDSCs, both in C26GM and EL-4 tumor models. Previous in vivo experiments using similar dosage and schedule of VSSP suggested that VSSP-MDSCs could display a reduced functional activity because VSSP potentiated Ag-specific CTL responses (27). These results suggest that MDSCs recruited during acute exposure to VSSP might exert a less suppressive function than that of counterparts induced during a chronic inflammation and tumor growth. The residual suppressive capacity of VSSP-MDSCs seemed to be more dependent on Nos than Arg, in contrast with tumor-induced MDSCs in which both Arg and Nos might play a role (15, 32, 33). Moreover, whereas *Nos3* was more upregulated than *Nos1* or *Nos2* in VSSP-MDSCs compared with that in tumor-free

CD11b$^+$ cells, C26GM-induced CD11b$^+$ cells only upregulated *Nos2* expression. It was shown that Nos2 enzyme is more efficient than Nos3 isoform to generate NO (49), which may explain in part the reduced suppressive capacity of VSSP-MDSCs. Phenotypic characterization also demonstrated changes in the main subpopulations within VSSP-MDSCs, which could account for their reduced suppressive function. CD11b$^+$ cells isolated from the spleens of VSSP-treated tumor-free and tumor-bearing mice showed reduced Gr-1^{low} and F4/80$^+$IL-4Rα^+ subpopulations compared with those of tumor-induced MDSCs. It was recently advanced that Gr-1^{low} cell population possessed the main suppressive capacity (34, 50). The lower accumulation of F4/80$^+$IL-4Rα^+ cells in VSSP-MDSCs might be linked to their reduced inhibitory activity compared with that of tumor-induced MDSCs, as IL-4Rα is important for MDSC activity in vitro and in vivo (15). Zhu et al. (51) demonstrated that only a small population of CD11b$^+$Ly6C^{high} inflammatory monocytes can efficiently suppress T cell responses in an experimental autoimmune encephalomyelitis model. In contrast, VSSP induced a higher amount of CD11b$^+$Ly6C^{high} cells than EL-4 and C26GM tumors, but tumor-derived MDSCs had a superior suppressive activity. Thus, CD11b$^+$Ly6C^{high} cells might not be the population responsible for the efficient suppression of T cell responses exerted by MDSCs under different pathological conditions, and other subpopulations could exert suppression depending on the stimulus, type of tumor, or genetic background. Finally, VSSP inoculation in tumor-bearing mice generated a splenic CD11b$^+$ population with a reduced suppressive ability compared with that of tumor-associated counterparts, both in EL-4 and C26GM tumor models.

Further in vivo experiments corroborated the diminished function of VSSP-MDSCs and the ability of VSSP to modulate the suppressive activity of tumor-derived MDSCs. Adoptive transfer of tumor-induced MDSCs into tumor-free VSSP-treated mice demonstrated the capacity of this adjuvant to create a particular environment able to restrain their suppressive activity on T cell responses. Moreover, the positive effect of VSSP on tumor-induced MDSCs was shown to be dominant, as a reduced suppressive function was observed after EL-4+VSSP-MDSC adoptive transfer. VSSP inoculation in EG.7 tumor-bearing mice restored the IFN-γ secretion by adoptively transferred OT-I CD8$^+$ T cells to levels similar to those obtained in tumor-free mice. The restorative action of this adjuvant seems to be unique because DC vaccination was ineffective. In addition, VSSP and not poly I:C inoculation protected Ag-specific CTL response in EL-4 tumor-bearing mice. Although other mechanisms might contribute, it appears that the VSSP adjuvant activity could be associated with its capacity to promote differentiation of tumor-induced MDSCs into APCs, as demonstrated by the in vivo differentiation experiments. Previous results from Kusmartsev and Gabrilovich (52) showed that, when transferred into naive recipients, Gr-1$^+$ cells isolated from tumor-free mice differentiated in vivo more quickly than tumor-derived counterparts into functional DCs and macrophages, indicating a delay in the differentiation program of these tumor-induced MDSCs. Our results suggest that also MDSCs isolated from VSSP-treated tumor-bearing mice differentiated more rapidly into APCs than tumor-induced counterparts. Thus, immunization with VSSP could be a better choice than DC vaccination or poly I:C adjuvant to develop a potent immune response in immunocompromised tumor-bearing hosts.

CD11b$^+$ cells sorted from tumor infiltrate showed similar immunosuppressive properties in vitro on a per-cell basis, irrespective of adjuvant treatment. However, when tumor-induced splenic MDSCs were adoptively transferred to tumor-bearing mice inoculated with the adjuvant, these CD11b$^+$ cells migrated less to the tumor site, and those cells that effectively reached it differentiated to a greater extent toward MHCII$^+$ APCs. In addition,

a higher percentage of DCs lost CD11b marker in VSSP-inoculated mice. De Smedt et al. (37) demonstrated that DCs matured in vivo in response to LPS expressed high levels of B7 molecules and lost CD11b marker, and this phenotype was associated with a reduced capacity to process proteins and an increased efficiency to stimulate T cells. One hypothesis could be that VSSP administration modulates the tumor microenvironment facilitating the differentiation of the infiltrating MDSC population to mature APCs while the functionality of the remaining MDSCs is not changed. When VSSP was inoculated together with a TAA (either OVA or GM3), it caused a significant decrease in EG.7 and MCA203 tumor growth (Fig. 6A, 6B), confirming the antitumor efficacy of several vaccine candidates when admixed with VSSP adjuvant, previously demonstrated in other tumor models (4, 24–26). In contrast, administration of VSSP in tumor-bearing mice did not change tumor-growth kinetics in EL-4 and C26GM tumor models (Supplemental Fig. 8A–C), probably due to a low expression level of GM3 in the first case and an inappropriate exposure of this ganglioside on the surfaces of C26GM tumor cells (data not shown). These results suggest that modification of tumor-induced MDSCs by VSSP is not sufficient to change primary tumor development, and a simultaneous stimulation of an effector CTL response against TAAs is also needed.

Chemical compounds like NO-aspirin and phosphodiesterase-5 inhibitors (e.g., sildenafil, vardenafil, and tadalafil) can reduce MDSC function, restoring T cell function and improving efficacy of antitumoral treatments (53, 54). However, these inhibitors do not change MDSC accumulation. In contrast, inoculation of CpG adjuvant induces CD11b$^+$Gr-1$^+$ cell accumulation in the spleens of treated mice, which efficiently suppresses T cell-mediated alloreactivity and graft-versus-host disease in a murine model of allogeneic cell therapy (55). Our results with VSSP demonstrate that an increased frequency of MDSCs is not necessarily correlated with the strongest immunosuppression, as VSSP reduced the suppressive ability of tumor-induced MDSCs. Finally, this work indicates that VSSP could be a cancer vaccine adjuvant able to target tumor-induced immunosuppression while stimulating a potent immune response against tumor Ags.

Disclosures

The authors have no financial conflicts of interest.

References

1. Mocellin, S., S. Mandruzzato, V. Bronte, M. Lise, and D. Nitti. 2004. Part I: vaccines for solid tumours. *Lancet Oncol.* 5: 681–689.
2. Ostrand-Rosenberg, S. 2004. Animal models of tumor immunity, immunotherapy and cancer vaccines. *Curr. Opin. Immunol.* 16: 143–150.
3. Carr, A., Z. Mazorra, D. F. Alonso, C. Mesa, O. Valiente, D. E. Gomez, R. Perez, and L. E. Fernandez. 2001. A purified GM3 ganglioside conjugated vaccine induces specific, adjuvant-dependent and non-transient antitumour activity against B16 mouse melanoma in vitro and in vivo. *Melanoma Res.* 11: 219–227.
4. Gabri, M. R., Z. Mazorra, G. V. Ripoll, C. Mesa, L. E. Fernandez, D. E. Gomez, and D. F. Alonso. 2006. Complete antitumor protection by perioperative immunization with GM3/VSSP vaccine in a preclinical mouse melanoma model. *Clin. Cancer Res.* 12: 7092–7098.
5. Machiels, J. P., R. T. Reilly, L. A. Emens, A. M. Ercolini, R. Y. Lei, D. Weintraub, F. I. Okoye, and E. M. Jaffee. 2001. Cyclophosphamide, doxorubicin, and paclitaxel enhance the antitumor immune response of granulocyte/macrophage-colony stimulating factor-secreting whole-cell vaccines in HER-2/neu tolerized mice. *Cancer Res.* 61: 3689–3697.
6. Tatsumi, T., T. Takehara, T. Kanto, T. Miyagi, N. Kuzushita, Y. Sugimoto, M. Jinushi, A. Kasahara, Y. Sasaki, M. Hori, and N. Hayashi. 2001. Administration of interleukin-12 enhances the therapeutic efficacy of dendritic cell-based tumor vaccines in mouse hepatocellular carcinoma. *Cancer Res.* 61: 7563–7567.
7. Jonasch, E., C. Wood, P. Tamboli, L. C. Pagliaro, S. M. Tu, J. Kim, P. Srivastava, C. Perez, L. Isakov, and N. Tannir. 2008. Vaccination of metastatic renal cell carcinoma patients with autologous tumour-derived vitespen vaccine: clinical findings. *Br. J. Cancer* 98: 1336–1341.
8. Rosenberg, S. A., J. C. Yang, and N. P. Restifo. 2004. Cancer immunotherapy: moving beyond current vaccines. *Nat. Med.* 10: 909–915.

9. Small, E. J., P. F. Schellhammer, C. S. Higano, C. H. Redfern, J. J. Nemunaitis, F. H. Valone, S. S. Verjee, L. A. Jones, and R. M. Hershberg. 2006. Placebo-controlled phase III trial of immunologic therapy with sipuleucel-T (APC8015) in patients with metastatic, asymptomatic hormone refractory prostate cancer. *J. Clin. Oncol.* 24: 3089–3094.

10. Wood, C., P. Srivastava, R. Bukowski, L. Lacombe, A. I. Gorelov, S. Gorelov, P. Mulders, H. Zielinski, A. Hoos, F. Teofilovici, et al; C-100-12 RCC Study Group. 2008. An adjuvant autologous therapeutic vaccine (HSPPC-96; vitespen) versus observation alone for patients at high risk of recurrence after nephrectomy for renal cell carcinoma: a multicentre, open-label, randomised phase III trial. *Lancet* 372: 145–154.

11. Malmberg, K. J. 2004. Effective immunotherapy against cancer: a question of overcoming immune suppression and immune escape? *Cancer Immunol. Immunother.* 53: 879–892.

12. Sica, A., and V. Bronte. 2007. Altered macrophage differentiation and immune dysfunction in tumor development. *J. Clin. Invest.* 117: 1155–1166.

13. Sinha, P., V. K. Clements, S. K. Bunt, S. M. Albelda, and S. Ostrand-Rosenberg. 2007. Cross-talk between myeloid-derived suppressor cells and macrophages subverts tumor immunity toward a type 2 response. *J. Immunol.* 179: 977–983.

14. Zou, W. 2006. Regulatory T cells, tumour immunity and immunotherapy. *Nat. Rev. Immunol.* 6: 295–307.

15. Gallina, G., L. Dolcetti, P. Serafini, C. De Santo, I. Marigo, M. P. Colombo, G. Basso, F. Brombacher, I. Borrello, P. Zanovello, et al. 2006. Tumors induce a subset of inflammatory monocytes with immunosuppressive activity on CD8+ T cells. *J. Clin. Invest.* 116: 2777–2790.

16. Huang, B., P. Y. Pan, Q. Li, A. I. Sato, D. E. Levy, J. Bromberg, C. M. Divino, and S. H. Chen. 2006. Gr-1+CD115+ immature myeloid suppressor cells mediate the development of tumor-induced T regulatory cells and T-cell anergy in tumor-bearing host. *Cancer Res.* 66: 1123–1131.

17. Nagaraj, S., K. Gupta, V. Pisarev, L. Kinarsky, S. Sherman, L. Kang, D. L. Herber, J. Schneck, and D. I. Gabrilovich. 2007. Altered recognition of antigen is a mechanism of CD8+ T cell tolerance in cancer. *Nat. Med.* 13: 828–835.

18. Serafini, P., C. De Santo, I. Marigo, S. Cingarlini, L. Dolcetti, G. Gallina, P. Zanovello, and V. Bronte. 2004. Derangement of immune responses by myeloid suppressor cells. *Cancer Immunol. Immunother.* 53: 64–72.

19. Liu, C., S. Yu, J. Kappes, J. Wang, W. E. Grizzle, K. R. Zinn, and H. G. Zhang. 2007. Expansion of spleen myeloid suppressor cells represses NK cell cytotoxicity in tumor-bearing host. *Blood* 109: 4336–4342.

20. Suzuki, E., V. Kapoor, A. S. Jassar, L. R. Kaiser, and S. M. Albelda. 2005. Gemcitabine selectively eliminates splenic Gr-1+/CD11b+ myeloid suppressor cells in tumor-bearing animals and enhances antitumor immune activity. *Clin. Cancer Res.* 11: 6713–6721.

21. Bronte, V., and P. Zanovello. 2005. Regulation of immune responses by L-arginine metabolism. *Nat. Rev. Immunol.* 5: 641–654.

22. Gabrilovich, D. I., and S. Nagaraj. 2009. Myeloid-derived suppressor cells as regulators of the immune system. *Nat. Rev. Immunol.* 9: 162–174.

23. Estevez, F., A. Carr, L. Solorzano, O. Valiente, C. Mesa, O. Barroso, G. V. Sierra, and L. E. Fernandez. 1999. Enhancement of the immune response to poorly immunogenic gangliosides after incorporation into very small size proteoliposomes (VSSP). *Vaccine* 18: 190–197.

24. Carr, A., E. Rodríguez, Mdel. C. Arango, R. Camacho, M. Osorio, M. Gabri, G. Carrillo, Z. Valdés, Y. Bebelagua, R. Pérez, and L. E. Fernández. 2003. Immunotherapy of advanced breast cancer with a heterophilic ganglioside (NeuGcGM3) cancer vaccine. *J. Clin. Oncol.* 21: 1015–1021.

25. Ramírez, B. S., E. S. Pestana, G. G. Hidalgo, T. H. García, R. P. Rodríguez, A. Ullrich, and L. E. Férnandez. 2006. Active antimetastatic immunotherapy in Lewis lung carcinoma with self EGFR extracellular domain protein in VSSP adjuvant. *Int. J. Cancer* 119: 2190–2199.

26. Torréns, I., O. Mendoza, A. Batte, O. Reyes, L. E. Fernández, C. Mesa, and G. Guillén. 2005. Immunotherapy with CTL peptide and VSSP eradicated established human papillomavirus (HPV) type 16 E7-expressing tumors. *Vaccine* 23: 5768–5774.

27. Mesa, C., J. de León, and L. E. Fernández. 2006. Very small size proteoliposomes derived from *Neisseria meningitidis*: an effective adjuvant for generation of CTL responses to peptide and protein antigens. *Vaccine* 24: 2692–2699.

28. Mesa, C., J. De León, K. Rigley, and L. E. Fernández. 2004. Very small size proteoliposomes derived from *Neisseria meningitidis*: an effective adjuvant for Th1 induction and dendritic cell activation. *Vaccine* 22: 3045–3052.

29. Bronte, V., P. Serafini, C. De Santo, I. Marigo, V. Tosello, A. Mazzoni, D. M. Segal, C. Staib, M. Lowel, G. Sutter, et al. 2003. IL-4-induced arginase 1 suppresses alloreactive T cells in tumor-bearing mice. *J. Immunol.* 170: 270–278.

30. Lutz, M. B., N. Kukutsch, A. L. Ogilvie, S. Rössner, F. Koch, N. Romani, and G. Schuler. 1999. An advanced culture method for generating large quantities of highly pure dendritic cells from mouse bone marrow. *J. Immunol. Methods* 223: 77–92.

31. Kusmartsev, S., S. Nagaraj, and D. I. Gabrilovich. 2005. Tumor-associated CD8+ T cell tolerance induced by bone marrow-derived immature myeloid cells. *J. Immunol.* 175: 4583–4592.

32. Bronte, V., D. B. Chappell, E. Apolloni, A. Cabrelle, M. Wang, P. Hwu, and N. P. Restifo. 1999. Unopposed production of granulocyte-macrophage colony-stimulating factor by tumors inhibits CD8+ T cell responses by dysregulating antigen-presenting cell maturation. *J. Immunol.* 162: 5728–5737.

33. Kusmartsev, S., and D. I. Gabrilovich. 2005. STAT1 signaling regulates tumor-associated macrophage-mediated T cell deletion. *J. Immunol.* 174: 4880–4891.

34. Dolcetti, L., E. Peranzoni, S. Ugel, I. Marigo, A. Fernandez Gomez, C. Mesa, M. Geilich, G. Winkels, E. Traggiai, A. Casati, et al. 2010. Hierarchy of immunosuppressive strength among myeloid-derived suppressor cell subsets is determined by GM-CSF. *Eur. J. Immunol.* 40: 22–35.

35. Fujimoto, C., Y. Nakagawa, K. Ohara, and H. Takahashi. 2004. Polyriboinosinic polyribocytidylic acid [poly(I:C)]/TLR3 signaling allows class I processing of exogenous protein and induction of HIV-specific CD8+ cytotoxic T lymphocytes. *Int. Immunol.* 16: 55–63.

36. Ngoi, S. M., M. G. Tovey, and A. T. Vella. 2008. Targeting poly(I:C) to the TLR3-independent pathway boosts effector CD8 T cell differentiation through IFN-alpha/beta. *J. Immunol.* 181: 7670–7680.

37. De Smedt, T., B. Pajak, E. Muraille, L. Lespagnard, E. Heinen, P. De Baetselier, J. Urbain, O. Leo, and M. Moser. 1996. Regulation of dendritic cell numbers and maturation by lipopolysaccharide in vivo. *J. Exp. Med.* 184: 1413–1424.

38. Luft, T., K. C. Pang, E. Thomas, P. Hertzog, D. N. Hart, J. Trapani, and J. Cebon. 1998. Type I IFNs enhance the terminal differentiation of dendritic cells. *J. Immunol.* 161: 1947–1953.

39. Kurts, C. 2008. CD11c: not merely a murine DC marker, but also a useful vaccination target. *Eur. J. Immunol.* 38: 2072–2075.

40. Parmiani, G., C. Castelli, L. Pilla, M. Santinami, M. P. Colombo, and L. Rivoltini. 2007. Opposite immune functions of GM-CSF administered as vaccine adjuvant in cancer patients. *Ann. Oncol.* 18: 226–232.

41. Serafini, P., R. Carbley, K. A. Noonan, G. Tan, V. Bronte, and I. Borrello. 2004. High-dose granulocyte-macrophage colony-stimulating factor-producing vaccines impair the immune response through the recruitment of myeloid suppressor cells. *Cancer Res.* 64: 6337–6343.

42. Almand, B., J. I. Clark, E. Nikitina, J. van Beynen, N. R. English, S. C. Knight, D. P. Carbone, and D. I. Gabrilovich. 2001. Increased production of immature myeloid cells in cancer patients: a mechanism of immunosuppression in cancer. *J. Immunol.* 166: 678–689.

43. Nagaraj, S., and D. I. Gabrilovich. 2010. Myeloid-derived suppressor cells in human cancer. *Cancer J.* 16: 348–353.

44. Zea, A. H., P. C. Rodriguez, M. B. Atkins, C. Hernandez, S. Signoretti, J. Zabaleta, D. McDermott, D. Quiceno, A. Youmans, A. O'Neill, et al. 2005. Arginase-producing myeloid suppressor cells in renal cell carcinoma patients: a mechanism of tumor evasion. *Cancer Res.* 65: 3044–3048.

45. Brys, L., A. Beschin, G. Raes, G. H. Ghassabeh, W. Noël, J. Brandt, F. Brombacher, and P. De Baetselier. 2005. Reactive oxygen species and 12/15-lipoxygenase contribute to the antiproliferative capacity of alternatively activated myeloid cells elicited during helminth infection. *J. Immunol.* 174: 6095–6104.

46. Goñi, O., P. Alcaide, and M. Fresno. 2002. Immunosuppression during acute *Trypanosoma cruzi* infection: involvement of Ly6G (Gr1(+))CD11b(+)immature myeloid suppressor cells. *Int. Immunol.* 14: 1125–1134.

47. Birklé, S., G. Zeng, L. Gao, R. K. Yu, and J. Aubry. 2003. Role of tumor-associated gangliosides in cancer progression. *Biochimie* 85: 455–463.

48. Shurin, G. V., M. R. Shurin, S. Bykovskaia, J. Shogan, M. T. Lotze, and E. M. Barksdale, Jr. 2001. Neuroblastoma-derived gangliosides inhibit dendritic cell generation and function. *Cancer Res.* 61: 363–369.

49. Bogdan, C. 2001. Nitric oxide and the immune response. *Nat. Immunol.* 2: 907–916.

50. Movahedi, K., M. Guilliams, J. Van den Bossche, R. Van den Bergh, C. Gysemans, A. Beschin, P. De Baetselier, and J. A. Van Ginderachter. 2008. Identification of discrete tumor-induced myeloid-derived suppressor cell subpopulations with distinct T cell-suppressive activity. *Blood* 111: 4233–4244.

51. Zhu, B., Y. Bando, S. Xiao, K. Yang, A. C. Anderson, V. K. Kuchroo, and S. J. Khoury. 2007. CD11b+Ly-6C(hi) suppressive monocytes in experimental autoimmune encephalomyelitis. *J. Immunol.* 179: 5228–5237.

52. Kusmartsev, S., and D. I. Gabrilovich. 2003. Inhibition of myeloid cell differentiation in cancer: the role of reactive oxygen species. *J. Leukoc. Biol.* 74: 186–196.

53. De Santo, C., P. Serafini, I. Marigo, L. Dolcetti, M. Bolla, P. Del Soldato, C. Melani, C. Guiducci, M. P. Colombo, M. Iezzi, et al. 2005. Nitroaspirin corrects immune dysfunction in tumor-bearing hosts and promotes tumor eradication by cancer vaccination. *Proc. Natl. Acad. Sci. USA* 102: 4185–4190.

54. Serafini, P., K. Meckel, M. Kelso, K. Noonan, J. Califano, W. Koch, L. Dolcetti, V. Bronte, and I. Borrello. 2006. Phosphodiesterase-5 inhibition augments endogenous antitumor immunity by reducing myeloid-derived suppressor cell function. *J. Exp. Med.* 203: 2691–2702.

55. Morecki, S., Y. Gelfand, E. Yacovlev, O. Eizik, Y. Shabat, and S. Slavin. 2008. CpG-induced myeloid CD11b+Gr-1+ cells efficiently suppress T cell-mediated immunoreactivity and graft-versus-host disease in a murine model of allogeneic cell therapy. *Biol. Blood Marrow Transplant.* 14: 973–984.

Supplementary Figure legends

Figure S1. Schematic representation of the treatment protocols to evaluate *in vivo* suppression and differentiation of CD11b⁺ cells. (A-B) CD8⁺ T cells from CD45.2⁺ OT-I or CL4-Thy1.1⁺ transgenic mice (orange tag) were adoptively transferred (AT) i.v. into naïve CD45.1⁺ C57BL/6 or Thy1.2⁺ BALB/c recipient mice (grey tag). Two days later, these mice were vaccinated (pink tag and siringe) and within one hour, on day 0, and day 4, transferred with purified CD11b⁺ cells from different sources indicated on the blue tags. On day 10, cells from lymph nodes (LNs) were isolated, restimulated *in vitro* with specific or control peptides, and analyzed for the antigen-specific IFN-γ release by intracellular staining (ICS). In **(C)** no CD11b⁺ cells were transferred, instead EG.7 tumor cells were implanted six days before vaccination, as a source of natural induced CD11b⁺ cells. Scheme **(D)** represents the protocol followed to evaluate *in vivo* migration and differentiation of transferred CD11b⁺ cells isolated from EL-4 tumor-bearing, CD45.1⁺ congenic mice. Host mice, with a CD45.2⁺ phenotype, were also previously conditioned, as shown on oranges tags. On day 3 following adoptive transfer, the recipients' spleens, LNs, and tumors were collected and single cells suspension of all organs were analyzed by FACS.

Figure S2. Effect of VSSP treatment on the phenotype and functional capacity of EL-4-induced splenic MDSCs. EL-4 tumors were grown s.c. in C57BL/6 mice and both tumor-free and tumor-bearing mice were inoculated three times with VSSP. Another group of animals with tumors remained untreated. **(A)** CD11b⁺ cells were enriched from pools of spleens by magnetic microbeads and stained with the indicated antibodies. Values indicate the mean ± SD of the cell percentages from the data of two independent experiments. From top to bottom panel: FACS profile of CD11b⁺ cells from VSSP-treated tumor-free mice, EL-4 tumor-bearing mice, and mice with EL-4 tumors inoculated with VSSP. **(B)** To evaluate the inhibition of cytotoxic activity, CD8⁺ T cells from pmel-1 transgenic mice were co-cultured with CD11b⁺ cells (at

24% of total cells) in the presence of the specific peptide. Graph shows percentages of specific lysis, measured five days later by ^{51}Cr released, at graded effector cell dilutions. Data are represented as mean ± SD and illustrate the results from one experiment repeated with similar results.

Figure S3. Transient effect of VSSP on EL-4 tumor-induced MDSCs. C57BL/6 mice were s.c. inoculated with EL-4 tumor cells and further immunized with three doses of VSSP. **(A)** Mean ± SD of the percentage of splenic CD11b$^+$Gr-1$^+$ cells detected seven days after the last VSSP dose. Statistical analyses were performed with ANOVA and Tukey tests and the differences are symbolized by letters. **(B)** Suppressive capacity of MDSCs isolated from EL-4 tumor-bearing mice, treated or not with VSSP, seven days after the last adjuvant administration. Antigen-specific CD8$^+$ T cells were stimulated *in vivo* by immunizing naïve mice with 1 mg of OVA antigen admixed with poly I:C (Sigma, USA; 100 µg per mice), on days 9, 10 and 11. 4x10^5 splenocytes from OVA/poly I:C immunized mice were restimulated for 72 hours with SIINFEKL peptide in the presence or absence of 20% CD11b$^+$ cells and IFN-γ secretion was detected by ELISPOT assay. Statistically significant differences are indicated by diverse letters (Kruskal-Wallis and Dunnett tests).

Figure S4. Induction of antigen-specific CTL responses in EL-4 tumor-bearing mice by different adjuvants. EL-4 tumor cells were implanted s.c. in C57BL/6 mice that received two immunization schedules afterward. Tumor-bearing and tumor-free mice were immunized s.c. with three doses of OVA antigen (1 mg/mouse) admixed with either VSSP (days 4, 5, and 11) or poly I:C (PIC, days 9, 10, and 11). Poly I:C was administered at 100 µg/mouse. Two days after the last dose, mice were injected i.v. with equal amount of SIINFEKL-pulsed or control splenocytes differentially stained with CFSE. After 24 hours the total events corresponding to both fluorescent intensities in the spleens was determined by FACS and the percentage of specific lysis calculated according the formula: $100-(CFSE^{high}/CFSE^{low} \times 100)$. Graphs show
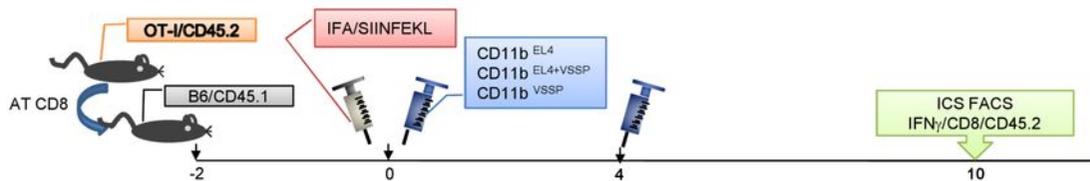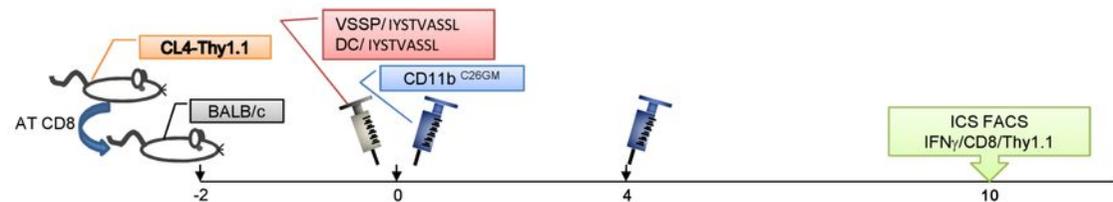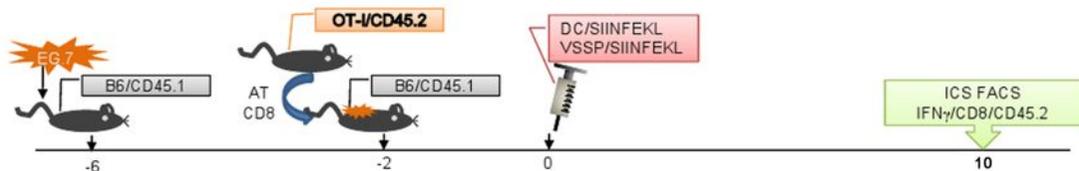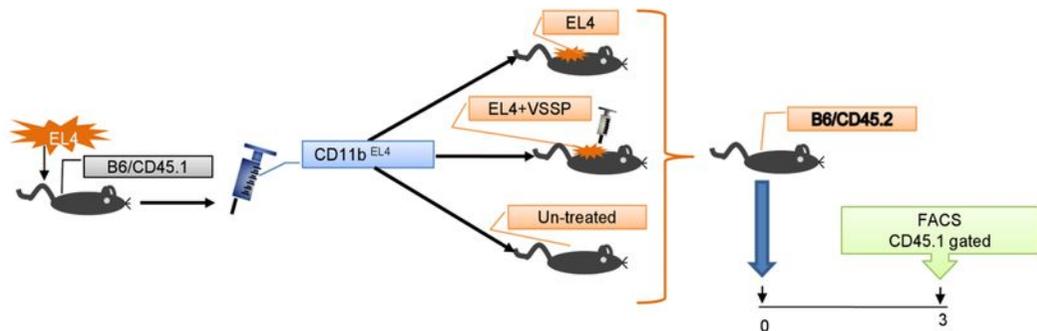
the specific lysis, as a percentage of the control (tumor-free mice), observed in mice treated with either OVA/VSSP **(A)** or OVA/poly I:C **(B)**. Data are represented as mean of three individual mice ± SD. Statistical analyses were performed with 2-tailed t test: [**] $p \leq 0.01$. Two experiments with similar results were performed.
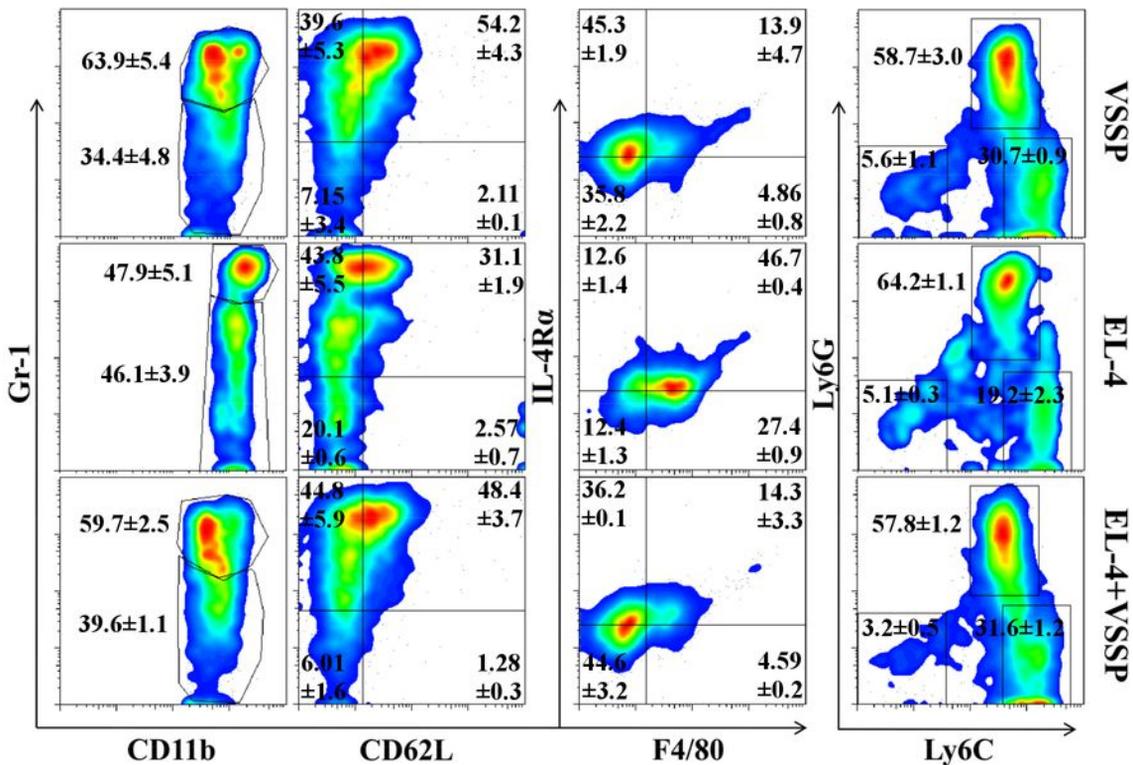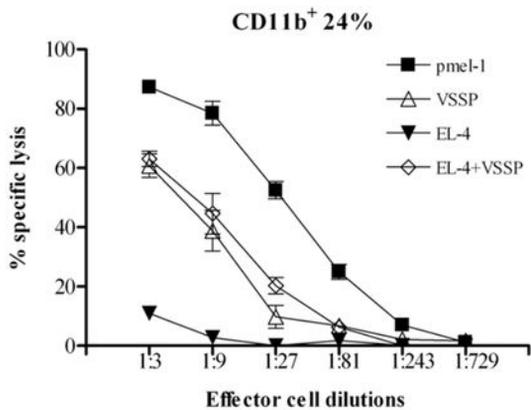
Figure S5. Phenotypic characterization of tumor-infiltrating CD11b$^+$ cells isolated from EL-4 tumor-bearing mice, treated or not with VSSP. EL-4 tumor cells were implanted s.c. in C57BL/6 mice that were next injected or not with three doses of VSSP. Two days after the last VSSP dose, mice were euthanized and CD11b$^+$ cells isolated from the tumor tissue. FACS characterization of tumor-infiltrating MDSCs isolated from both experimental groups was performed. Mean ± SD of the cell percentages obtained from two independent experiments are indicated.
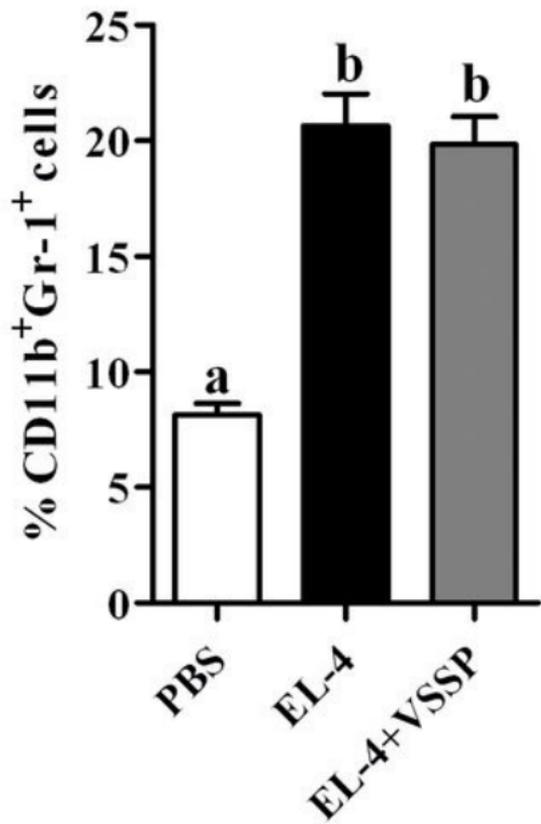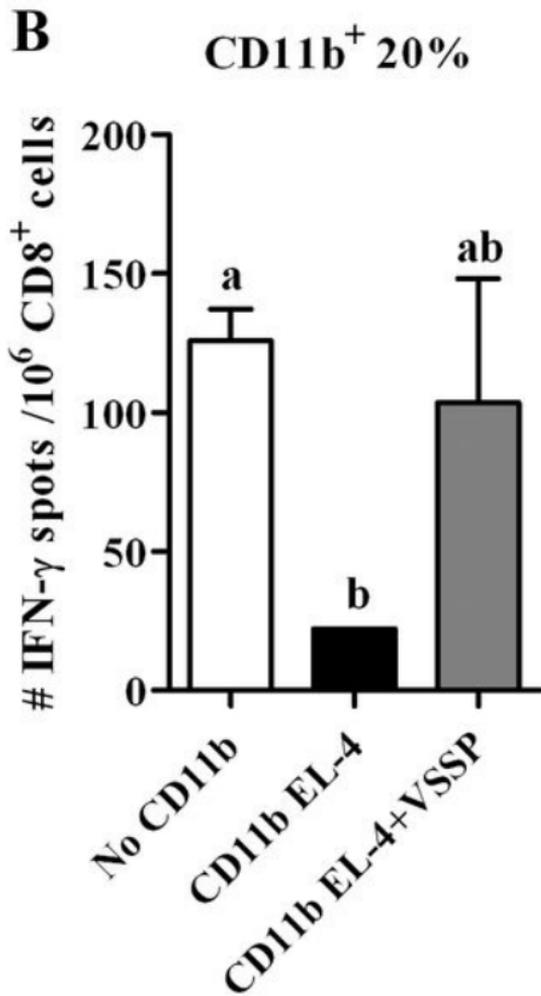
Figure S6. Changes in migration and differentiation patterns of tumor-induced MDSCs associated to VSSP administration. CD11b$^+$ cells isolated from the spleen of EL-4 tumor-bearing mice were transferred to differentially conditioned congenic mice (indicated on graphs). On day 3, adoptively transferred CD45.1$^+$ cells were analyzed by FACS. **(A and B)** Dot graphs represent migration of transferred CD11b$^+$ cells to LNs **(A)** and spleen **(B)**, measured as the number of CD45.1$^+$ cells per million of total cells. Also the phenotype of spleen-infiltrating CD45.1$^+$ cells was evaluated by MHCII/F4/80 **(C and E)** and CD11c/CD11b **(D and F)** staining. In dot graphs **(A-D)** individual mice evaluations are plotted and horizontal lines represent the group's mean. Statistically significant differences ($p \leq 0.05$) were detected by ANOVA and Tukey tests and are indicated with different letters. Figures **E** and **F** show contour graphs where quadrants were individually set on positions where the staining with isotype control antibodies was less that 1 %. This experiment is representative of two identical.
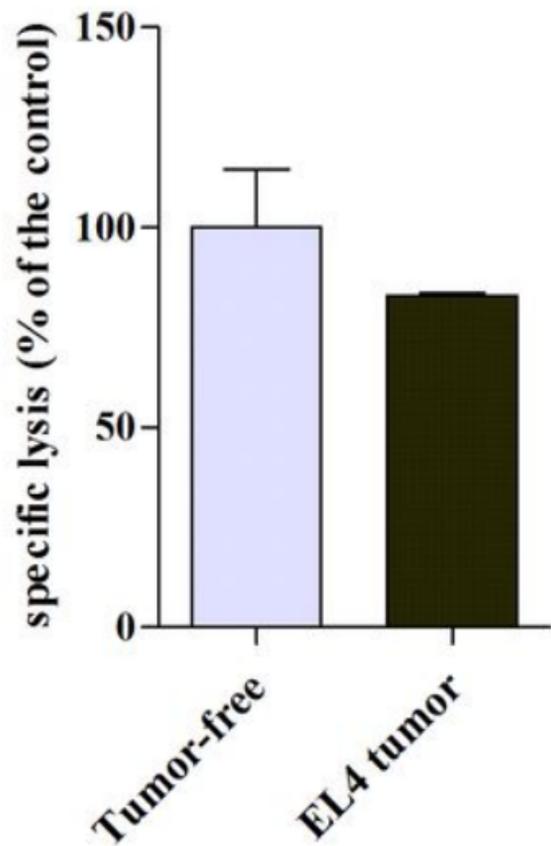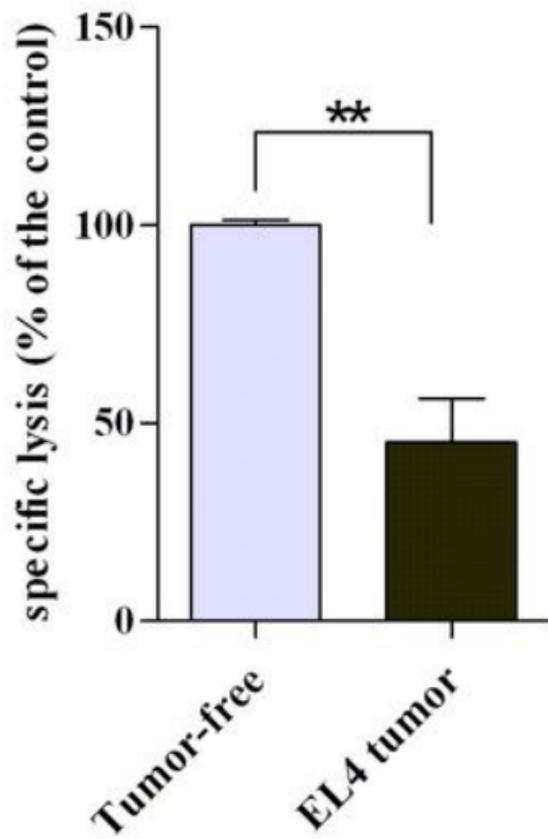
Figure S7. Influence of the different VSSP components on MDSC accumulation. C57BL/6 mice were inoculated s.c. with three doses of either VSSP or OMP (Outer Membrane Proteins from *Neisseria meningitidis*), at equal protein amount. Two days after the last dose, spleens were extracted and splenocytes analyzed by flow cytometry to determine the frequency of $CD11b^+Gr-1^+$ cells. **(A)** Percentage of $CD11b^+Gr-1^+$ cells in the spleen of treated mice. Data are expressed as mean ± SD (n=5 mice). Statistical analyses were performed with Kruskal-Wallis and Dunnett tests. Diverse letters represent statistically significant differences ($p \leq 0.05$) of the group's mean. **(B)** Contour graphs show the double staining of splenocytes with anti-CD11b and anti-Gr-1 specific antibodies from three individual representative mice per group. Two experiments with similar results were performed.

Figure S8. Effect of VSSP administration on tumor growth kinetics. BALB/c or C57BL/6 mice were challenged s.c. on day 0 with C26GM and EL-4 tumor cells, respectively. VSSP was administered s.c. on days 1, 2 and 7 in BALB/c mice, while in C57BL/6 the doses were given on days 4, 5 and 11. Tumor largest perpendicular diameters were measured with a caliper on the indicated days and tumor volume calculated with the formula: *π/6 x length x width²*. Dot graphs show individual mice per group at 6 **(A)** and 9 **(B)** days after C26GM tumor challenge and horizontal lines represent the group's mean. Statistical comparison was performed by Student's *t* test and *p* values are indicated in the graphs. **(C)** Tumor progression in EL-4 tumor-bearing mice treated or not with VSSP. Data are expressed as mean ± SD from seven individual mice. Statistical analyses were conducted for each day data using Mann-Whitney's U test and no differences were found. These experiments were repeated three times with similar results.
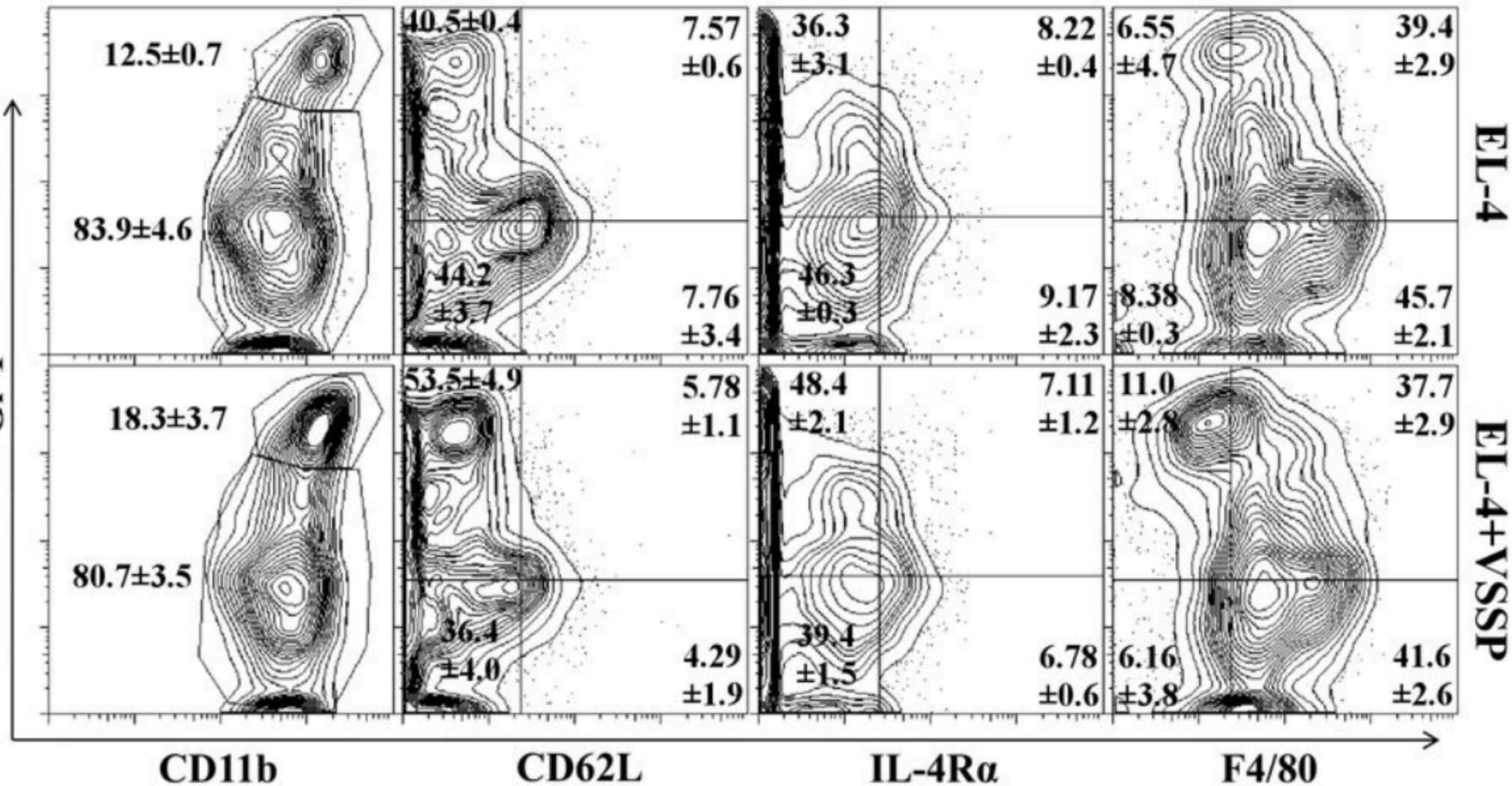
A

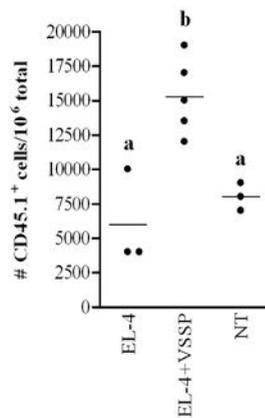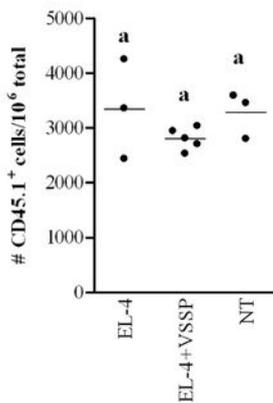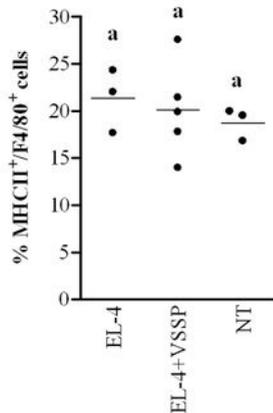OT-I/CD45.2 — IFA/SIINFEKL

AT CD8

B6/CD45.1

CD11b^EL4
CD11b^EL4+VSSP
CD11b^VSSP

ICS FACS
IFNγ/CD8/CD45.2

-2   0   4   10

B

CL4-Thy1.1 — VSSP/IYSTVASSL
DC/IYSTVASSL

AT CD8

BALB/c

CD11b^C26GM

ICS FACS
IFNγ/CD8/Thy1.1

-2   0   4   10

C

EG7

B6/CD45.1

OT-I/CD45.2

AT CD8

B6/CD45.1

DC/SIINFEKL
VSSP/SIINFEKL

ICS FACS
IFNγ/CD8/CD45.2

-6   -2   0   10

D

EL4

B6/CD45.1

CD11b^EL4

EL4

EL4+VSSP

Un-treated

B6/CD45.2

FACS
CD45.1 gated

0   3

A

(Top to bottom rows: VSSP, EL-4, EL-4+VSSP)

Column 1 (Gr-1 vs CD11b):
- VSSP: 63.9±5.4, 34.4±4.8
- EL-4: 47.9±5.1, 46.1±3.9
- EL-4+VSSP: 59.7±2.5, 39.6±1.1

Column 2 (CD62L):
- VSSP: 39.6±5.3, 54.2±4.3, 7.15±3.4, 2.11±0.1
- EL-4: 43.8±5.5, 31.1±1.9, 20.1±0.6, 2.57±0.7
- EL-4+VSSP: 44.8±5.9, 48.4±3.7, 6.01±1.6, 1.28±0.3

Column 3 (IL-4Rα vs F4/80):
- VSSP: 45.3±1.9, 13.9±4.7, 35.8±2.2, 4.86±0.8
- EL-4: 12.6±1.4, 46.7±0.4, 12.4±1.3, 27.4±0.9
- EL-4+VSSP: 36.2±0.1, 14.3±3.3, 44.6±3.2, 4.59±0.2

Column 4 (Ly6G vs Ly6C):
- VSSP: 58.7±3.0, 5.6±1.1, 30.7±0.9
- EL-4: 64.2±1.1, 5.1±0.3, 19.2±2.3
- EL-4+VSSP: 57.8±1.2, 3.2±0.5, 31.6±1.2

B

CD11b⁺ 24%

Legend:
- ■ pmel-1
- △ VSSP
- ▼ EL-4
- ◇ EL-4+VSSP

% specific lysis vs Effector cell dilutions (1:3, 1:9, 1:27, 1:81, 1:243, 1:729)

A

% CD11b$^+$Gr-1$^+$ cells

PBS (a), EL-4 (b), EL-4+VSSP (b)

B CD11b$^+$ 20%

IFN-γ spots /10^6 CD8$^+$ cells

No CD11b (a), CD11b EL-4 (b), CD11b EL-4+VSSP (ab)

A OVA/VSSP

B OVA/PIC

A # CD45.1$^+$ cells/10^6 total

B # CD45.1$^+$ cells/10^6 total

C % MHCII$^+$/F4/80$^+$ cells

D % of total CD11c$^+$ cells

Groups: EL-4, EL-4+VSSP, NT

E MHCII vs F4/80 — EL-4, EL-4+VSSP, NT

F CD11b vs CD11c — EL-4, EL-4+VSSP, NT

A Day6

B Day9

C